8-2020

Empirical Modeling of Used Nuclear Fuel Radiation Emissions for Safeguards Purposes

Amanda M. Bachmann
University of Tennessee, Knoxville, abachma2@vols.utk.edu

To the Graduate Council:

I am submitting herewith a thesis written by Amanda M. Bachmann entitled "Empirical Modeling of Used Nuclear Fuel Radiation Emissions for Safeguards Purposes." I have examined the final electronic copy of this thesis for form and content and recommend that it be accepted in partial fulfillment of the requirements for the degree of Master of Science, with a major in Nuclear Engineering.

Jamie B. Coble, Major Professor

We have read this thesis and recommend its acceptance:

Steven E. Skutnik, Richard T. Wood

Accepted for the Council:
Dixie L. Thompson

Vice Provost and Dean of the Graduate School

(Original signatures are on file with official student records.)

Empirical Modeling of Used Nuclear Fuel Radiation Emissions for Safeguards Purposes

A Thesis Presented for the

Masters of Science

Degree

The University of Tennessee, Knoxville

Amanda Marie Bachmann

August 2020

Acknowledgements

I would like to thank Dr. Jamie Coble, my major professor, for her continued and immense support and guidance over my 5 years at the University of Tennessee, Knoxville. Without her I would not have my current career aspirations. I would also like to thank Dr. Steven Skutnik and Dr. Richard Wood, my master's committee members, for their support during my education and research. I would also like to thank my family and partner for all of their continued support of my education and professional endeavors.

The work presented here was funded in part by the RISER program. The Research and Instructional Strategies for Engineering Retention (RISER) at the University of Tennessee, Knoxville was funded by the National Science Foundation (NSF) through the Science, Technology, Engineering, and Mathematics Talent Expansion Program (STEP) award number 1068103.

Abstract

For nuclear nonproliferation safeguards, the ability to characterize used nuclear fuel (UNF) is a vital process. Fuel characterization allows for independent verification by inspectors of operator declarations of the special nuclear material flow and nuclear related activities within a facility, and an estimation of fissile material remaining in a fuel assembly. Current methods to verify this information rely heavily on non-destructive assay techniques, such as gamma spectroscopy and neutron detection measurements. While these measurements are effective tools for estimating a specific characteristic of the fuel, such as burnup or cooling time, they often require an accurate estimation of a select few isotopes in the fuel. This requirement means that the characterization is based on a very small amount of information that is contained in radiation emissions. To help overcome this limitation, this work investigates the use of empirical modeling to predict the burnup, initial enrichment, and cooling time of a Westinghouse 17x17 UNF assembly. This technique utilizes the entire spectrum of gamma emissions and gross neutron counts to predict each output to explore the full suite of information contained in these signatures. Three primary parametric modeling techniques are investigated for their performance in modeling this system: Ordinary Least Squares Regression (OLS), Principal Component Regression (PCR), and Partial Least Squares Regression (PLS). The models created are evaluated based on their root mean square percent error and condition number. The uncertainty of the best performing model is then quantified to understand the prediction interval of the predicted characterization and how this compares to the uncertainty of current measurement and characterization techniques.

The PLS models are able to provide the best predictions while being stable. The PCR models have a consistent trade-off between accurate prediction results and stability. The OLS model provides fairly accurate results but is highly unstable due to correlations in the input data. The best model is the PLS model based on cross validation because it is stable, yields the lowest RMSPE values for burnup and enrichment predictions, and yields the second lowest percent of cooling time predictions that are more than 1 year away from the actual value.

When used with the validation data set, this model yields RMSPE values of 0.42%, 1.39% and 4.61% for the burnup, enrichment, and cooling time, respectively. The total uncertainty of the predictions of this model are calculated to be 0.220 GWd/MTU, 0.051% U-235, and 0.694 years, for the burnup, enrichment, and cooling time, respectively.

Table of Contents

List of Figures

Chapter 1

Introduction

For any peaceful nuclear fuel cycle, nonproliferation safeguards are an important aspect. Safeguards help to account for special nuclear material (SNM) quantities and identify diversions of SNM within a declared nuclear facility. They are required for any state that is a signatory of the Nuclear Nonproliferation Treaty with the United Nations [3]. A large emphasis of nonproliferation safeguards is on the ability to independently verify fissile material quantities and operator declarations at a facility [4]. The ability to perform these tasks provides confidence that State-supplied information is truthful and accurate, and that material has not been diverted. Current methods to verify this information with regards to used nuclear fuel (UNF) after it is discharged from a reactor are based on the ability to characterize the fuel.

Characteristics of UNF that are of interest to safeguards are the burnup, initial enrichment, and the cooling time because they can be related to the fissile material of the fuel [5]. Current methods to verify these characteristics primarily consist of quantifying the amount of specific isotopes, such as Cs-137, Eu-154, and Cm-244, in the fuel through gamma or neutron emissions. These measurements can be limited by the half-life, fission yield, or emission energy of the isotopes to be quantified. To address these limitations, empirical modeling has been suggested as a way to use multiple isotopes or emissions to predict the characteristics of the UNF for process monitoring [6, 7]. By utilizing multiple points of information, such as multiple isotope concentrations or energy bins of a gamma spectrum, more observable information about the fuel can be used to characterize the fuel. This work explores how empirical modeling can be applied to the verification of UNF characteristics for nuclear safeguards purposes. Multiple modeling techniques are investigated to identify

the best technique for this application based on simulated data. The performance of each model created is characterized based on its prediction accuracy and stability. Gamma and neutron emissions from UNF are considered as model inputs, to limit the need to quantify a single or subset of isotopes. The outputs of the models are the burnup, initial enrichment, and cooling time of the fuel.

1.1 Organization of the Document

The next chapter discusses background information about nuclear safeguards, current methods to verify fuel characteristics, and provides an overview of empirical modeling. The third chapter describes the procedure to generate the input and output space of the data used to train and evaluate the models and outlines modeling techniques explored and the performance metrics for each model. The three chapters that follow explain the calculations of a specific regression technique, how the technique is used, and the results for that technique. The seventh chapter then summarizes the results of all models created, selects the best model, and performs uncertainty analysis on that model. The final chapter provides conclusions and suggestions for future work.

Chapter 2

Background

2.1 Nuclear Nonproliferation Safeguards

The primary goal of international safeguards, from the perspective of the International Atomic Energy Agency (IAEA), is to provide "timely detection of diversion of significant quantities of nuclear material from peaceful nuclear activities" to the creation of nuclear explosives or weapons [4]. Violations of safeguards agreements can come in various forms, including the diversion of special nuclear material, or the presence of undeclared nuclear material and activities [8]. Therefore, the ability to detect each of these activities is vital to the implementation of nuclear safeguards.

To detect a diversion of special nuclear material, material control and accountancy measures are often put into place. These have the primary focus of monitoring the fissile material, such as plutonium, in the fuel. Due to the irradiation of the fuel, measurements of radiation signatures of the plutonium that could directly quantify its amount are masked by the radiation signatures of fission products and other actinides. Therefore, the fissile material content must be estimated through means of other characteristics of the fuel [5]. One of the characteristics of interest to estimate the fissile content in UNF is the burnup of the fuel, or the integrated energy released from the fission of heavy metal [9]. Accurate knowledge the total burnup of the fuel can provide estimations of the build-up of Pu-239 and Pu-241, fissile isotopes of plutonium, in the UNF. Relating the burnup to the plutonium content in the fuel can be performed through indirect determination using empirical relationships with fissile content or through active neutron interrogations to induce fission [5]. The empirical

relationship calculations are often performed via computer codes, such as CINDER [10] or ORIGEN [11]. The neutron interrogation method requires a neutron source, such as Cf-252, and compares the interrogated neutron signal to a background measurement to determine the neutron multiplication factor. These measurements can be taken with systems such as the Californium Interrogation Prompt Neutron (CIPN) instrument [12], and are primarily limited by the availability and strength of the neutron source. Since the fissile material in UNF decays over time, it is also important to know the cooling time of the fuel, or how much time has passed since it has been discharged from the reactor. The cooling time is a required parameter for the calculation of the concentration of any isotope based on radiation signatures [9]. Based on this information, the cooling time is an important fuel characteristic to verify because it informs the decay of the fissile material and any isotopes used to estimate their concentration. A third parameter of importance for safeguards is the initial enrichment of the UNF. When combined with the burnup of the fuel, this parameter can inform inspectors of the remaining amount of uranium that the UNF should contain and the plutonium content, since this is a function of the initial enrichment.

To detect the presence of undeclared nuclear materials and activities, records are kept of material movement and operations of a declared facility [13]. To verify these records, routine inspections at nuclear facilities are carried out to collect information about compliance with safeguards agreements. Independent verification of these records informs the IAEA of the accuracy of records and the likelihood that material is being concealed from the Agency. This is of greater importance for a closed fuel cycle, in which UNF is reprocessed. The reprocessing step separates the fissile material in the fuel from the other materials, which increases the proliferation risk of the material since the fissile material is in a purified form. Verifying the fissile content of the UNF can inform inspectors of the fissile content that should be present at a reprocessing facility and help to perform material balances. The need to develop methods to verify declarations and conditions of the UNF in a closed fuel cycle has been outlined by Pacific Northwest National Laboratory [14]. One of the declared goals of verification methods is the ability to quantify the total plutonium concentration within 5%.

2.2 Current UNF Characterization Techniques

Measurements used for nuclear safeguards are typically described as either destructive assay (DA) or nondestructive assay (NDA) [15]. DA measurements are defined by their

consumption of the sample being measured, while NDA measurements do not. DA measurements will typically yield a more precise result, but NDA measurements are preferred for safeguards inspections because they can often be done without any alteration of the assembly, do not require additional resources, and are often quicker to perform [15].

Two common NDA measurements used for UNF characterization are gamma and neutron counting measurements, which can be correlated to information about the fuel [16]. Using a gamma spectra, the initial concentration of the emitting isotope (N_i^0) can be estimated from the measured activity (A_{ij}), the branching ratio of that emission (B_j), decay constant of the isotope (λ_i), cooling time (T_c), and the detector efficiency (ϵ_j), as shown in Eq. 2.1 [9].

$$N_i^0 = \frac{A_{ij} * e^{\lambda_i * T_c}}{\lambda_i * \epsilon_j * B_j} \tag{2.1}$$

Isotopes that are used for this process are typically fission products that have a high yield and emit high energy gammas that can easily be detected. The exact isotope used depends on the characteristic and the level of accuracy needed. Neutron emissions from UNF after the first few months of cooling time are from the spontaneous fission and (α,n) reactions, both of which are dependent on the transuranic element concentrations. The gross neutron rate is then correlated to the desired characteristic to verify operator declarations.

To characterize the burnup of UNF, one of the most common isotopes used is Cs-137 for a variety of reasons. First, Cs-137 has a known linear correlation to burnup, which provides a simple way to relate the two quantities. Second, it has a long half-life (about 30 years), meaning it does not quickly decay away and can be measured in older fuel assemblies. Third, Cs-137 emits a high enough energy gamma that can penetrate through any self-shielding effects of the fuel assembly and the photopeak can be distinguished from background noise and radiation. Finally, Cs-137 has an approximately equal yield when it is produced through fission of U-235 and fission of Pu-239 [5], meaning that as Pu-239 begins to fission at higher burnup of the fuel, there is no significant change in the Cs-137 production rate to deviate from the linear relationship. While these are all qualities that make Cs-137 an excellent burnup indicator, this measurement requires that an absolute count rate is obtained to ensure that the activity of the isotope in Eq. 2.1 is known to great accuracy. To acquire this, all aspects of the system must be known: the detector efficiencies, signal to noise ratios, background radiation levels, and corrections for any other emissions that would be detected in the same energy bin. It is difficult to directly quantify some of these values, and it takes additional

time to correct for them, increasing the amount of time and work that is needed for this method to provide accurate results.

Other gamma emitting isotopes used in a similar manner to estimate the burnup of UNF include Cs-134 and Eu-154 [17, 9]. These isotopes have a power relationship with the burnup [18], as opposed to the linear relationship for Cs-137, and are produced from neutron capture or other reactions as opposed to a direct fission product. Cs-134 as a burnup indicator is limited by its half-life (about 2 years), which means that once UNF is taken out of a spent fuel pool (usually about 5 years), there is less than a quarter of the original amount present in the fuel. The gamma signal from this isotope will be not as distinguishable from the background signal by the time UNF is removed from the spent fuel pool. Eu-154 has a longer half-life than Cs-134 (about 8 years) and will remain as a viable signature in the fuel for much longer.

The use of a single gamma emitting isotope to estimate the burnup of the assembly is limited by the ability to take a measurement and account for all detector effects, such as geometric efficiencies and instrument noise. To remove the need for the quantification of all of these parameters, ratios of gamma emitters can be used for estimating the burnup [5]. Typical ratios include Cs-134 or Eu-154 to Cs-137. By using a ratio, the detector effects can be assumed to be the same for the measurements, and a less precise measurement can be used to garner the same amount of information about the assembly. However, some of the quantities required for an absolute count rate are still required when using isotopic ratios, such as background count rates. Isotopic ratios also require knowledge of the other parameters present in Eq. 2.1, as well as the fission yield of each isotope to be used in UNF characterization [9].

Passive neutron measurements can also be used to verify burnup levels and are primarily based on emissions from curium in the fuel. Curium is the primary neutron emitter in UNF, accounting for about 95% of neutron emissions after the first 10 years of cooling time [16]. Due to the strength of curium as a neutron emitter, a passive neutron count will be proportional to the total curium concentration [9]. The concentration is then related to the burnup to the fourth power, an empirical relationship based on the rate of neutron captures required to produce the curium [5]. Using curium has limitations since not much of it is produced in low enriched uranium (LEU) fuel, on the order of 20 g/tU [5, 9], and it has a relatively short half-life (18.1 years for Cm-244 and 0.45 years for Cm-242). This means that this method of verifying the burnup of UNF requires accurate knowledge of the cooling time, to account for the decay of the curium, and the initial enrichment, since Cm-244 is

produced through neutron capture of U-238. Methods to estimate the initial enrichment and cooling time will be discussed later in this section. This counting method is also affected by any neutron poisons present, such as boron in a spent fuel pool, since neutron poisons will reduce the neutron counts measured by the detector [16].

To combine the information obtained from gamma and neutron measurements, the fork detector has been developed and used for UNF characterization. Fork detectors are bi-pronged instruments with an ionization chamber and two fission chambers on each side to provide simultaneous total gamma and total neutron counting [5]. One of the fission chambers on each side has a cadmium coating, while the other is bare, to provide a comparison of thermal and fast neutron counts. The detector is placed around the fuel assembly taking measurements from two sides and can be moved along the assembly to provide an axial measurement. The measurement of a single assembly takes 5-7 minutes, and can characterize the burnup of the assembly to with 5% of the declared value [5]. While this a simple and quick way to take gamma and neutron measurements, it is still limited by the required calculations to convert these signatures to the desired characteristics and often relies on correction factors in these calculations based on declared values, removing the ability to independently verify the information [16]. The fork detector also requires an identical reference assembly of known characteristics for calibration of the detector [16], which can be difficult to obtain during an inspection.

The enrichment of nuclear fuel is fairly easy to characterize if the fuel has not been irradiated. Gamma spectroscopy can be used to quantify the intensity of the 185.7 keV gamma emitted by U-235 relative to the intensity of the 1001 keV gamma emitted from U-238 [19]. This measurement can be used with a NaI(Tl) detector with a single channel analyzer (SCA) around the photopeak and another SCA above the energy of the photopeak to allow for background correction in the spectrum. Neutron emissions can also be used to characterize the enrichment of fresh fuel. The U-234 in the fuel, a daughter product of U-238, is the strongest alpha emitter present. The emitted alphas can then cause (α, n) reactions with the F-19 from the UF_6 gas. This reaction rate is proportional to the amount of U-234, which is also related to the U-235 concentration in the system [19]. This method is not able to discern an exact enrichment in LEU (<5%), but it can easily distinguish between LEU and highly enriched uranium (>20%).

While these methods are very useful for safeguards verification at other points in the fuel cycle, they are not applicable to UNF due to the build-up of fission products and other actinides that have stronger emissions and conceal the signatures used for fresh fuel. It

has been proposed to characterize the initial enrichment of UNF by measuring the induced neutron emissions of the fuel when it is exposed to an external source [17]. By using a pulsed source, the spontaneous neutron emissions of the fuel can be measured and subtracted out from the measured sum of the spontaneous and induced neutron emissions. This method has not been employed in a real facility, due to the high cost of obtaining and using a pulse neutron source. The work by Favalli et al., in addition to the empirical relationships for burnup and cooling time, developed an empirical relationship between the burnup and initial enrichment of fuel [20]. This was shown to be fairly accurate, resulting in values typically within 5% of the declared value, but this relationship is dependent on accurate knowledge of the burnup of the fuel. The parameters are for this relationship are based on a functional fit to data, and therefore have associated errors that can limit the relationship's accuracy. Other than these methods, no methods have been established to characterize the initial enrichment of UNF from radiation signatures.

To estimate the cooling time, single and ratios of isotopic concentrations can be used, similar to how they are used to verify the burnup [9]. Example isotopes that are used for this measurement include Pr-144, Rh-106/Cs-137, and Cs-134/Eu-154. Pr-144 reaches a saturation activity after two years of irradiation and is thus not sensitive to the burnup of the fuel. Both isotopic ratios are nearly independent of the burnup due to similar relationships between the isotopic concentrations and the burnup of the fuel. The insensitivity to burnup allows for these isotopic markers to be relatively constant at the time of discharge and provide information about the cooling time of the fuel based on their concentration. The cooling time is then calculated based on the decay constant, current concentration, and initial concentration, as shown in Eq. 2.2 for use of a single isotope and Eq. 2.3 for use of a ratio [9].

$$T_c = \frac{1}{\lambda_i} * \ln\left(\frac{N_i^0}{N_i}\right) \tag{2.2}$$

$$T_c = \frac{1}{\lambda_2 - \lambda_1} * \ln\left(\frac{N_1}{N_2}\right) + \frac{1}{\lambda_2 - \lambda_1} * \ln\left(\frac{N_2^0}{N_1^0}\right) \tag{2.3}$$

Based on these equations, this method of characterizing the cooling time of UNF is limited by the ability to measure the activity of the isotopes and calculate their concentration at the time of discharge and at the time of measurement. There are some semi-empirical relationships similar to these equations that can be used with the concentration of Cs-134

and/or Cs-137 or Eu-154 [18]. These relationships are similar to Eqs. 2.2 and 2.3, but replace the initial and current concentrations with the ratio of a calibration constant multiplied by the initial concentration to the gamma intensity. While these relationships are able to estimate the cooling time using the same measurements that are used for burnup verification, establishing the calibration constant requires multiple well-characterized fuel assemblies.

The measurements discussed in this section are able to accurately characterize UNF, but they each have their own limitations. Most are entirely based on an accurate measurement of the concentration of a single or select few isotopes based on known correlations with the fuel characteristics and their radiation emission intensities. The techniques explored in this work hope to overcome this limitation by providing a way to estimate the burnup, initial enrichment, and cooling time of the fuel based on the entire emitted gamma spectrum and the total neutron counts.

2.3 Empirical Modeling

Empirical modeling is the use of data to model the behavior of a system, as opposed to first principles and physics based models. This type of modeling can have several advantages, specifically when the first principles of a system are not known or are very complicated to model. There are two primary types of empirical models: parametric and non-parametric models. Parametric models are constrained to a specified function form, such as linear, and utilize the same set of parameters across the entire range of observations to predict each new observation [21]. Parametric models are considered a global model because all observations are used to calculate the regression coefficients. Non-parametric models calculate new regression coefficients to relate each new observation to similar ones in the training data set. Non-parametric models are considered a local model because they utilize only observations close to the one being predicted to calculate the regression coefficients. For this work, only parametric models are considered. First, these models are primarily what has been used for previous fuel characterization efforts [6, 22, 23] and it is desired to provide a comparison of how commonly used modeling techniques perform using the specified inputs and outputs. Second, the input space of this work is fairly large, and it is expected to become computationally expensive to compare the distance between every observation in the training data set and each new query to be predicted.

A common issue encountered when performing empirical modeling of a multidimensional data set is multicollinearity, or high correlation between input variables. Multicollinearity in the input data means that independent variables to the model can actually be described by linear combinations of other independent variables, reducing the rank of the matrix, the amount of information contained by the input data, and can make the system under-determined. The reduced rank of the matrix can introduce issues of the stability of the matrix inversion part of a regression procedure.

2.3.1 Methods to Reduce Dimensionality

To help overcome the issue of multicollinearity, multiple dimensionality reduction techniques have been developed to transform a data set into a latent variable (LV), or unobserved variables, space. Methods of dimensionality reduction include Reduced-rank Regression [24], Principal Component Regression [25], and Continuum Regression [26]. Each of these methods utilize a transformation of the input data into a LV space based on a specified objective function. These objective functions can include minimizing the square error of predictions, as in reduced rank regression, or maximizing the variance in one direction of the input data, as in Principal Component Regression. In the LV space, a subset of the variables can be used to perform the regression, [27]. If all of the LVs are used, then the regression coefficients found are the same as that of using all of the variables in the original space.

When using a dimensionality reduction technique, there are a variety of methods to select the number of LVs to use. A common method to inform this decision is cross validation, which can generally be described as the selection of a model parameter such that it minimizes a loss function of the model [1]. Model parameters can include the number or subset of variables to use, a smoothing coefficient, or a combination of parameters. The loss function is typically an error estimation, such as root mean square error or residual sum of square errors. An example of cross validation is shown in Figure 2.1 [1]. This figure shows how the Mean Square Error (MSE_q) and cross validatory assessment of the parameter used for cross validation ($\mathrm{C}^{\dagger}$) as a function of the number of variables.

The optimization is typically performed using a subset of the data that is not the same subset used to create the model. For example, a training data set is used to calculate the regression coefficients, and the predictions of a testing data set are used with cross validation to select the model parameter that optimizes the results. The minimum loss function can be calculated directly by comparing different parameter values or visually determined based

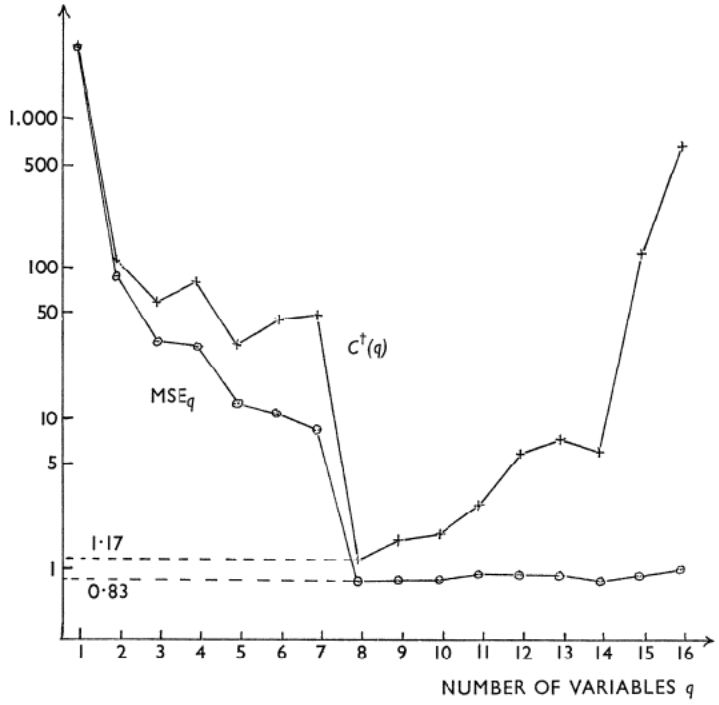

Figure 2.1: Example of cross validation to determine the number of variables to use based on Mean Square Error (MSE_q) and cross validatory assessment of the parameter used for cross validation ($C^{\dagger}$) [1].

on a figure of the loss as a function of the parameter value. While the direct calculation can be computationally automated, the visual inspection allows for expert opinion to determine if a different value should be used. Examples of this include using a fewer number of latent variables if the error appears to flatten. While the lowest error may be in the middle of the flat section, it may be desired to use the number of variables where the curve flattens to create a simpler model based on intuition.

A second common method is Akaike Information Criteria (AIC) [28]. AIC is an information criterion to describe the difference between the estimated and true probability functions that describe the loss function of a parameter estimate. It is calculated as shown in Eq. 2.4, in which $L(\hat{\theta})$ is the log maximum likelihood estimate and k is the degrees of freedom of the model.

$$AIC = -2L(\hat{\theta}) + 2k \tag{2.4}$$

$L(\hat{\theta})$ can be calculated as the average variance lost for each LV that is not used. Using AIC allows for the loss function to describe a lack of fit and a lack of parsimony. In practice, this provides an estimate of the model parameter that should be used for a model with multiple alternatives. This is done by calculating the AIC value of the model with each number of parameters available, then selecting the parameter that yields the lowest value. Since this method optimizes a loss function, it can be thought of as a form of cross validation based on information criteria instead of statistical predictions. AIC can be applied to factor analysis, PCA, and various multiple regression methods [28].

A third common method to determine the number of variables to use is a scree plot [29]. This is a visual method based on the identification of a large change in the graph of a function of the number of variables used. The exact function used is typically a latent root of the variable, which could be described as the eigenvalue of a PC or the amount of variance explained by an LV. The large change in slope is indicative of a lack of significant information in the subsequent variables. While this method does not require any additional calculations, there is not always a well-defined slope change in the plot used, as shown in Figure 2.2 [2], which increases the difficulty in identifying the proper number of variables to use.

2.3.2 Application to Safeguards

With regards to modeling of UNF, empirical modeling has been to a variety of purposes. There has been extensive work on its application for process monitoring in reprocessing facilities through the Multi-Isotope Process (MIP) Monitor [22]. The MIP Monitor consists of gamma detectors around a reprocessing facility to monitor for changes in the gamma signatures as the fuel undergoes changes. Multivariate analysis is applied to the signatures to detect any unexpected variations that would suggest a diversion is taking place. By applying hierarchical cluster analysis (HCA), PCA, and PLS on simulated gamma spectra, normal operations were clustered separate from off-normal operations of acid concentrations and burnup levels of the fuel were predicted to within 3.5% [22]. The MIP Monitor can also utilize measured gamma spectra to estimate the concentration of three isotopes that would be present in UNF [30]. By using PCA and PLS, the activity of modified button sources from gamma standards of Co-57, Eu-152, and Am-241 were identified to within 6% of the

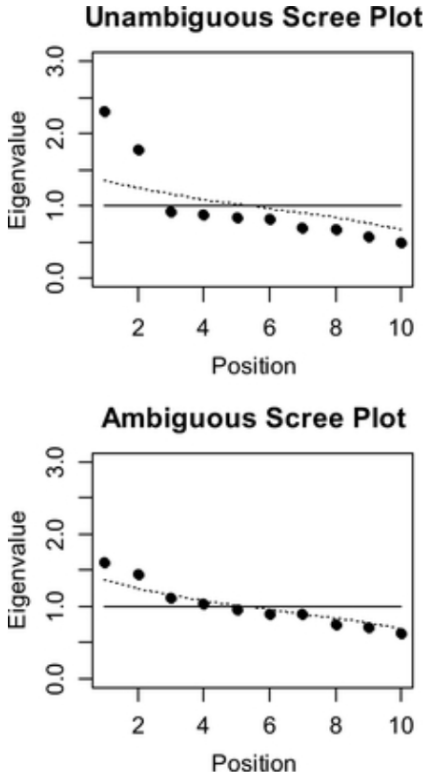

Figure 2.2: Examples of scree plots [2]. The bottom shows an example with no significant change in slope.

measured activity. Since these measurements are from a controlled sample, these results are likely more accurate than what could be obtained from the gamma spectroscopy of a UNF assembly. The multivariate analysis of the MIP Monitor was then used with signatures from physical boiling water reactor (BWR) assemblies, to investigate how these methods perform with physical measurements [31]. PLS models were built to predict the acid concentration and burnup based on the gamma spectrum taken from the fuel while in the organic extract of aqueous reprocessing. The predictions of the acid concentration mostly have low relative error, $< 10\%$, but the errors reach as high as 106.4%. The burnup prediction model, which was constructed based on Leave-One-Out cross validation, predicted the burnup within 2.5%. It was also explored how the 662 keV energy peak from Cs-137 impacts these results by comparing the performance of PLS models without this energy bin and a model based solely on this peak across multiple energy bins. The model without the peak performs slightly better than the original model, with predictions less than 2.25%. The model based solely on

the 662 keV peak performs worse, with most of the predictions having an error of about 4%. The model without the 662 keV peak uses 2 LVs, while the model based on the 662 keV peak uses 3 LVs, since multiple energy bins span the width of the peak. While the results of the 662 keV peak model are worse than the model without this peak, they are similar to what has previously been seen by using the Cs-137 correlation to burnup. While the MIP Monitor shows the ability of multivariate analysis to provide information about the UNF while it is being reprocessed, it does not provide any information about the fuel assembly before it is dismantled and placed in nitric acid. The work done to highlight the use of gamma spectra to estimate isotope concentrations was performed under very controlled conditions using samples of just those isotopes which would increase the accuracy of the predictions since there are no other signatures to interfere with those from the isotopes of interest.

To extend the capabilities of empirical modeling based on gamma spectra in the MIP Monitor, simulated measured gamma spectra were used as inputs to directly predict the characteristics of three types of boiling water reactor (BWR) UNF assemblies and three types of pressurized water reactor (PWR) UNF assemblies before they undergoes chemical separation [7]. This would allow for verification of operator declarations before the reprocessing begins, which can inform expectations of the signatures observed later in the process stream. PLS was exclusively used, with modifications, for the classification of the fuel type and the estimation of the burnup, initial enrichment, and cooling time. Modifications made to PLS include discriminant analysis for the reactor type classification and using locally weighted regression within the LV space for the other fuel characteristics. The authors also compared the accuracy of different procedures of performing the predictions and classifications, showing that characterizing the reactor type first has the greatest impact on characteristic estimation. For each of the model algorithms used, the reactor type had a 0% misclassification rate, the burnup, initial enrichment, and cooling time predictions were predicted within 0.15%, 3%, and 4% when the reactor type was classified first and within 0.5%, 11%, and 9% when it was not, respectively. While this work expands the capabilities of using gamma spectra to characterize UNF and show that knowing the type of reactor has a large impact on the accuracy of the predicted characteristics, it utilizes a small space for the cooling time and makes no adjustments for realistic characteristic combinations, such as a high burnup and low initial enrichment.

In addition to UNF characterization based on gamma spectra, isotopic concentrations have been used as model inputs to estimate fuel parameters [6, 23, 32]. Using isotopic concentrations as the input allows for the identification of additional nuclides that are related to these characteristics. Dayman et al. built two primary models: one to identify the type

of light water reactor and one to predict the burnup of the fuel [6]. The first was built using classifier algorithms such as k-Nearest Neighbors and linear discriminant analysis. The second model was built using PLS. To determine which nuclides should be used as inputs to each of the models, specifically the 200 isotopes most correlated to each of the outputs, feature selection was employed. The resulting models were able to correctly classify the type of reactor with 0% misclassification and predict the burnup value of the fuel within 0.1%. While this model has better accuracy in predicting the burnup of the fuel than the one based on the gamma spectrum [7], it has been explored for only this characteristic, while the gamma spectrum model has been explored for its predictions of the initial enrichment and cooling time as well. This model also relies on the ability to measure the concentration of 200 isotopes in the fuel, which is not expected to be possible to do during an inspection without the use of destructive assay measurements. Therefore, this model does not utilize a realistic input space.

Hellesen et al. used only the concentrations of 12 select isotopes in their model to predict the burnup, initial enrichment, and cooling time of pressurized water reactor (PWR) fuel [23]. The isotopes were broken into three groups, based on their half-life, to be used to predict characteristics of fuel within one of three age ranges, less than 1 year, 1-10 years, 10-20 years. PCA was used with each of these groups to predict the cooling time, and PLS was used to predict the burnup and initial enrichment of the fuel with an estimated cooling time. When applied to two sample fuel assemblies, the characteristics are well predicted for a fuel assembly with a cooling time of 5.4 years. However, there were larger errors for each of the parameters for a fuel assembly of cooling time 14.3 years due to the decrease in the variation of signatures and non-uniqueness of the solution space at higher cooling times. The predicted values were farther away from the actual value and the standard deviation on each of the predictions was larger. This work expanded the ability of isotope concentrations to predict additional characteristics, namely the initial enrichment and cooling time, and showed how PCA and PLS can be used together for these predictions. However, this model is shown to be very limited for longer cooling times, since there are fewer isotopes to use in characterizing such fuel. Both this work and the work by Dayman et al. are restricted by the use of isotopic concentrations to characterize UNF, which can be difficult to measuring using only NDA measurements and are shown to be limited for fuel of longer cooling time.

Charlton et al. examined specifically noble gas concentrations, namely Kr and Xe, produced during fission of commercial fuel to classify the reactor type and estimate the burnup of the fuel [32]. These noble gases are common fission products that are produced in relation to the isotope fissioning, the power level, and the neutron spectrum of the reactor. Therefore,

their concentrations can be correlated to the burnup. This method compares a database of the ratios of stable isotopes of Kr and Xe as a function of burnup to a sample taken from the fuel and processed through a mass spectrometer. The sample would be collected "on-stack" from the reprocessing facility during the decladding and dismantling of the assembly [32]. By coupling this comparison with Bayesian and Principal Component Analysis (PCA)/PCR analysis, the burnup of the fuel can be estimated. Samples taken must be corrected for the natural Xe-129, Kr-78, and Kr-80 present in the air before any analysis can be done. The Bayesian analysis involves comparing the measured ratios to the those contained in the database and determining which set of parameters most closely matches the data. PCA is used to compare the measured data to the clusters of to identify the reactor type, then PCR is used to estimate the burnup of the fuel. Both methods are used to enhance the robustness of the system. This method is limited to use at a reprocessing facility, due to the need to dismantle and dissolve the fuel assembly to release the noble gases. It also requires the use of a unique, high-precision mass spectrometer to measure the concentrations of the gases due to their low concentrations. It is unclear if this equipment can be brought on site for an inspection, or if it must remain in a laboratory and samples be transported to the mass spectrometer. Mass spectrometry is also not an NDA measurement technique, as it will destroy the sample, therefore this work would not qualify if NDA measurements are required.

Finally, Grape et al. explored how random forest algorithms, a non-parametric modeling technique, can be used with NDA signatures to predict UNF characteristics [33]. The NDA signatures used include fission product activities, the sum of fission product activities, total Cherenkov light intensity, and early die-away time. The fission product activities are related to their concentrations and the gamma emissions from the fuel, so these inputs are very similar to what has previously been used. The early die-away time is related to the decrease in a neutron population in the fuel, so its use attempts to incorporate information from the neutron signatures of the fuel into the model. By comparing different combinations of these inputs, the best predictions come when the fission product activities, the total Cherenkov light intensity and the early die-away time are used, with the largest impact being on the initial enrichment predictions. This suggests that the use of a neutron signature will lead to more accurate results overall, especially in the initial enrichment, as Hellesen et al. suggested [23]. It is observed that the gamma related NDA signatures still provide accurate results for fuel with a cooling time of less than 10 years. This work demonstrates how a non-parametric model performs in the characterization of UNF based on gamma and neutron

NDA signatures. However, this work uses inputs related to specific isotope concentrations, so it suffers from the same limitations as the other works.

These applications of empirical modeling to parameter estimation in UNF show that this can be an accurate method of characterizing UNF. There are a number of ways that these techniques can be used to characterize UNF: predicting isotopic concentrations based on a gamma spectrum or characterizing UNF based on a gamma spectrum or multiple isotopic concentrations. There is a strong emphasis on the use of PLS to perform quantitative predictions, with other methods used for clustering and feature identification. There is not much comparison of the use of different methods to perform the quantitative predictions. A comparison of different empirical modeling methods would provide reasoning for why PLS has primarily been the method of choice and highlight some of its strengths. In addition, there is limited work on how neutron signatures can impact UNF characterization and the small amount available shows promising results.

Chapter 3

Methodology

This work develops and compares multivariate techniques and models to predict characteristics of UNF that are important for safeguards evaluation of the back end of the nuclear fuel cycle. The inputs to each model are the radiation emissions of the UNF and the predicted characteristics (the outputs) are the burnup, initial enrichment, and cooling time of the fuel. The radiation emissions include the entire gamma spectrum and gross neutron counts from the fuel. The gamma spectrum is used based on the abundance of isotopes that are connected to the burnup [5], the improved accuracy of the use of multiple gamma emitting isotopes to define a set of unique fuel characteristics [34], and the accuracy of this input in previous modeling work [7]. The neutron counts are used because it has not been used in previous multivariate modeling efforts, it has been suggested as a logical extension of gamma spectra based models [23], and the use of an NDA measurement related to the neutron population in previous models has increased the accuracy of predicted characteristics [33]. The fuel characteristics were chosen based on commonly used characteristics during safeguards inspections and characteristics that have been modeled previously [7, 23]. The initial enrichment is of particular interested since there are no current NDA measurements in place to quantify it. The largest application of the models in this work is the verification of operator declarations of reactor operations and the characteristics of fuel being transported between facilities.

The output space was specified first, then the radiation signatures were simulated based on the output space. All observations for the data are for a Westinghouse 17x17 PWR fuel assembly. A single assembly type is used based on previous comparisons of models using multiple assembly types and models that are based on a single assembly type [7, 6]. It was

shown that predictions of fuel characteristics have improved accuracy when the assembly type is known. This characteristic can also more easily be verified during an inspection and was therefore not used as an output of the models. This assembly type was chosen because it is one of the most commonly used fuel assembly models in the U.S., and it is one of the simplest to model. All of the simulations consisted of 3 cycles of length 540 days at 100% power. The first two cycles are followed by 30 days of down time, and the third cycle is followed by the specified length of the cooling time. This was done to provide a realistic simulation of normal operations at a plant in the U.S. By using the same irradiation history for each observation, with the exception of the power level, this methodology does not account for any irregular operations, such as forced outages, or extended irradiations that would impact the emissions and their relation to each of the characteristics. It was also assumed that one metric ton of heavy metal is used.

The fuel characteristics chosen are based on common operations and normal operations of PWRs in the U.S., with additional space on both sides to ensure that the model is as inclusive as possible. The burnup space ranges from 20-70 GWd/MTU, in increments of 5 GWd/MTU. The enrichment of the fuel was calculated based on the burnup value according to Eq. 3.1 [20].

$$EN = 0.31 * BU^{0.65} \tag{3.1}$$

The enrichment was related to the burnup because they are often linked in commercial operations; if a fuel is intended to be burned for longer it will typically be enriched more to allow for the higher burnup. The relationship used allows for a more realistic enrichment space and correlation between these variables that would be observed in fuel. The relationship used assumes that the reactor operators are running the reactor to us the fuel most efficiently. To provide robustness for this assumption, a range of +/- 5 and 10% around this calculated value is used. The additional values also help to reduce the correlation between the burnup and enrichment and increase the stability of each model. The cooling times consist of 5, 6, 7, 8, 9, 10, 12.5, 15, 20, 25, and 30 years. The bin sizes for the cooling time varies based on the exponential nature of radioactive decay and are based on expected ages of fuel when they leave a reactor site.

The radiation signatures were simulated through the ORIGEN-ARP modules of SCALE [11]. The gamma spectra consist of 1024 energy bins, ranging from 100 keV to 4 MeV. Examples of the simulated spectra as a function of energy are shown in Figure 3.1. Since the gamma

spectra used for this work is the emissions from the fuel, it does not include any detector features, such as a Compton continuum, the Compton edge, or a Gaussian photopeak. It only features line peaks at the emission energy and does not necessarily reflect what can be measured during an inspection.

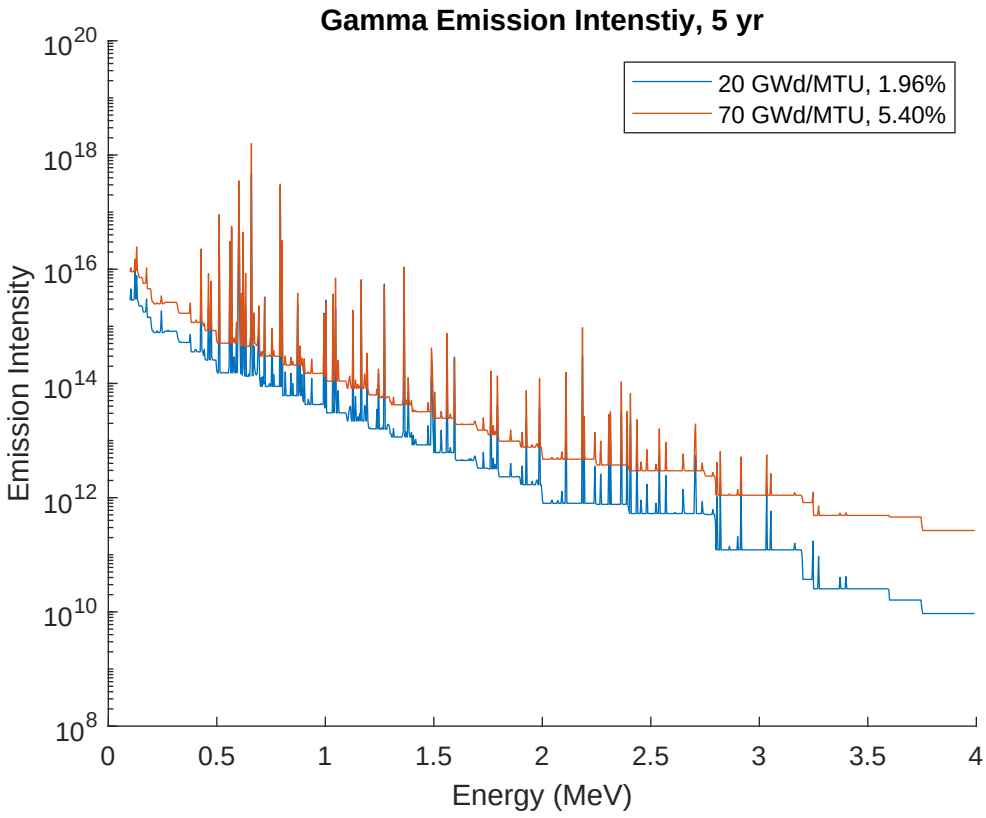

Figure 3.1: Simulated gamma spectra for the lowest burnup, lowest enrichment and highest burnup, highest enrichment combinations at 5 years cooling time.

Due to the increased difficulty of neutron spectroscopy in the field, it is desired to not have this be a limiting feature of use of the models. Therefore, it was decided to use a gross neutron emission count, as opposed to binned energy ranges like the gamma counts. This also prevents any added complexity that would be introduced by incorporating more highly correlated data into the input space.

Using these different parameters, the input of the model is a 605×1025 matrix, with each bin of the gamma spectra and the neutron counts as the input variables. The output matrix

is 605 × 3, with each of the desired characteristics as the variables. The data set was divided randomly into three sets; a training set with 302 observations, a testing set with 151 observations, and a validation set with 152 observations. The random data division prevents any relation between adjacent observations from being incorporated into the models. The training and testing sets were used to build and optimize models using three regression techniques: Ordinary Least Squares Regression (OLS), Principal Component Regression (PCR), and Partial Least Squares Regression (PLS).

Dimensionality reduction techniques (PCR and PLS) are a primary focus of the techniques used because the input data set contains more variables than observations, which means that it is an under-determined system. They are also included because the input variables are highly correlated due to multiple emissions from the same isotopes, branching ratios, decay chains, and fission yields. When the dimensionality reduction techniques are used, the maximum number of variables that can be used is the minimum between the number of variables minus one and the number of observations in the training data set. The restriction based on the number of variables is due to the production of the same results as OLS if all of the latent variables are used. The restriction on the number of latent variables ensures that the system is not under-determined, and a solution of regression coefficients can be calculated. Based on these restrictions, the maximum number of latent variables that can be used for PCR or PLS is 302 variables. This holds true for all models created using these techniques, unless otherwise specified. Use of these methods requires that any transformed data is standardized, or mean centered and scaled to a standard deviation of one. This ensures that the directions and distances found for the variances present in the input data are of meaning, as opposed to indicating the distance from the origin to the center of the data.

The models will be evaluated based on their root mean square percent error (RMSPE) and their condition number, with the best model used to predict the validation data set and quantify the uncertainty of the model. The RMSPE will be calculated based on Eq. 3.2, in which y is the actual data and $\hat{y}$ is the predicted data.

$$RMSPE = \frac{\sqrt{mean((y - \hat{y})^2)}}{mean(y)} \times 100 \tag{3.2}$$

A percent error is used for equal comparison across each of the outputs, since they are each on different scales. There has been an established goal of measuring plutonium content to within 5% of the actual value [14], which corresponds to approximately an equal percent error

in the burnup. Based on this information, it is desired to predict burnup and enrichment, since it is closely tied to the burnup, to within 5%. For the cooling time, an error of ± 1 year has been identified of being able to discriminate between discharge cycles for a given assembly [34], so that target is applied to this work. These requirements will be balanced with obtaining the lowest RMSPE value of the predictions, because that will help to indicate if there is a significant variance in the predicted values.

The condition number of a model will be used to evaluate the stability of each model. This metric describes how small perturbations in the data are amplified in predictions, as shown in Eq. 3.3 [35].

$$\frac{\|\delta f\|}{\|f\|} \leq ConditionNumber \times \frac{\|\delta y\|}{\|y\|} \tag{3.3}$$

The calculation of a condition number can be performed in a variety of methods. It is generally calculated as the ratio of the largest singular value of the matrix being inverted in linear regression to the smallest singular value of that matrix. Since the singular values of a matrix are related to the eigenvalues of a matrix, they can also be calculated as the ratio of the maximum eigenvalue to the minimum eigenvalue of that matrix, as shown in Eq. 3.4. If a subset of the variables are used in the model, such as in PCR, then the eigenvalues used for this calculation are adjusted to only consider the variables used in the model.

$$Cond = \frac{\lambda_{max}}{\lambda_{min}} \tag{3.4}$$

The minimum value of a condition number is 1, which corresponds to the inversion of a scalar value. It represents that small changes in the input data set will cause at most an equal change in the output predictions. Large condition numbers represent that small changes in the input data will lead to large differences in the fitted parameters, which can lead to large increases or decreases in the prediction error of a second data set. Therefore, large condition numbers are not favored since they mean that there is large variance in the predictions. For this work, an absolute maximum threshold of 100 will be placed on the condition number for a model to be considered stable. This is based on common practices of empirical modeling and will be used to help ensure consistency on the performance of the selected model.

Once the best model is selected, it will be used to predict the validation data set and quantify the uncertainty of the model. The uncertainty of the model allows for better understanding

of the limitations of how the model can be applied to real world safeguards inspections. The model uncertainty can be used to determine is a prediction is statistically different than the declared value.

Model uncertainty has three primary components: noise variance, prediction variance, and bias [36]. Noise variance is an irreducible error that comes from the variance of the input data. This variance is a function of the ability to measure the inputs and random noise in these measurements. Since all of the radiation signatures were simulated and the output variables were all hand selected numbers, it is assumed that there is no noise variance in these models. Prediction variance is the expected variance between the actual outputs and the predicted outputs. While this can be calculated in a similar manner to normal error propagation, for this work it is calculated using Monte Carlo sampling of the predictions. This procedure builds a number of prototypic models using different subsets of the input data, uses that subset to predict the output data, then calculates the variance of these subsets of output predictions. 500 samples of 100 data points of the validation data set are used to calculate this value. Finally, the bias of the model is the average difference between the actual and predicted outputs. It provides information on how much a model under or over predicts the outputs. To calculate the bias of the model, a direct estimation method is used: the bias is the mean of the difference between the actual output values and the predicted outputs, as shown in Eq. 3.5.

$$Bias = mean(y - \hat{y}) \tag{3.5}$$

The total uncertainty of a model is the square root of the sum of the prediction variance, $\sigma^2_{\hat{y}}$, and the square of the bias, as shown in Eq. 3.6.

$$Uncertainty = \sqrt{\sigma^2_{\hat{y}} + bias^2} \tag{3.6}$$

The total uncertainty is the standard deviation of each prediction, and in units of the value being predicted. The total uncertainty of a model can be used to develop prediction intervals and test for anomalous measurements.

Chapter 4

Ordinary Least Squares Regression

The first modeling technique is Ordinary Least Squares Regression (OLS), which finds the best linear combination of coefficients to relate the input variables to the output, as shown in Eq. 4.1 [37]. In this equation, Y is the output data that is being predicted, X is the input data, β is the matrix of regression coefficients, and E is the noise.

$$Y = X * \beta + E \tag{4.1}$$

Using the training data set, the matrix of regression coefficients is solved for, such that they minimize the error between Y and $X * \beta$. This calculation can theoretically be done by multiplying both sides of Eq. 4.1 by the inverse of X, but this assumes that X is a nonsingular, invertible matrix, which may not always be true. To avoid this assumption, β can also be solved for by using a pseudoinverse to solve Eq. 4.1. The pseudoinverse is derived from the minimization of the mean square error between Y and $X * \beta$, and is calculated by multiplying both sides by the transpose of the input matrix, then multiplying by $(X^T X)^{-1}$. This results in Eq. 4.2 to solve for β.

$$\beta = (X^T X)^{-1} X^T Y \tag{4.2}$$

The calculated β can then be used in Eq. 4.1 to predict the output of future observations, such as the testing data set, and calculate the error between these predictions and the actual output.

The use of a pseudoinverse allows for the coefficients to be solved for when the input matrix is not square or full-rank, which are both conditions of matrix inversion. While the pseudoinverse meets these conditions, the calculation of β still requires a matrix inversion step. This step introduces five assumptions about the system and the data:

1. The system being modeled is linear
2. The inputs are measured perfectly
3. All important variables are available
4. The inputs are independent
5. The noise in the output is homoscedastic, normally distributed, and independent

For the data used in this work, item 1 is assumed to not be true. With respect to the burnup of the fuel, some isotopes have a known linear relationship with burnup, such as Cs-137, but there are many isotopes that have a nonlinear relationship with burnup, such as Cs-134, Cm-244, and Eu-154 [5]. The enrichment values have a logarithmic relationship to the burnup, and therefore any relationships between the emissions and the burnup will be tied to the enrichment in this work, with additional nonlinearities introduced from the relationship between the burnup and enrichment. The cooling time is known to have an exponential decay relationship to the intensity of radiation emissions, based on decay laws, and therefore will not readily meet this assumption. Item 2 is assumed to be true because the input data has been simulated and therefore will not contain any signal noise or measurement error. Item 3 is assumed to be true because these are the targeted measurements of this work. Item 4 is known to not be true, since there are known correlations between the energy bins of a gamma spectra and neutron counts, such as multiple emissions and decay chains. Finally, item 5 is known to hold true, since none of the outputs contain noise. Despite the known issues of meeting these assumptions, this method is still investigated to provide insights into how well these assumptions are actually met and because it is a foundational technique that is utilized by the other techniques in this work.

OLS was initially performed using the entire training data set, but due to the high correlations between input variables even the pseudoinverse is a reduced rank, singular matrix. This means that the entire data set cannot be used to perform OLS. Therefore, the amount of correlation in the input data was reduced in order to provide a full rank pseudoinverse for matrix inversion. Correlations were removed based on the correlation

coefficient, or the ratio of the covariance of the variables to the maximum possible covariance, of each pair of variables in the input data. The higher the correlation coefficient, the more correlated the variables are, with a value of 1 indicating that they are perfectly correlated. A threshold of 0.99 was applied to the correlation coefficients, so that only those correlated to all other variables less than that will be used for OLS. Although the threshold is relatively high, and the remaining variables will still be correlated, the high correlations in the data left only 12 variables and placing the threshold lower could leave not enough variables to yield a set of coefficients.

The 12 variables left in the collapsed data set were all gamma energy bins, since the neutron counts are perfectly correlated to some of the higher energy bins. The neutron emissions are primarily coming from the spontaneous fission of Cm-244 in the fuel, which also releases higher energy gamma rays. The 12 remaining energy bins are all below 0.9 MeV, and represent only the most uncorrelated bins, and represent no correlation to the output or what energy bins may be the best predictors of each characteristic. The collapsed data still contains energy bins for important photopeaks. The seventh variable, energy bin 109 captures the 511 keV peak for a positron annihilation, and the tenth variable, energy bin 148, captures the 662 keV photopeak of the Cs-137 decay. There are 3 energy bins between 662 keV and 900 keV, which are the energy bins that would be distinguished best from background when taking a physical measurement. The lack of perfectly correlated variables helps to ensure that assumption 4 is better met by the model and will have better stability.

The collapsing of the variables is performed for any data set used with OLS, keeping all of the observations. The training data set is used to calculate β in Eq. 4.1 and the condition number of the model, then the testing data set is used with the calculated β to make a set of predictions and calculate their RMSPE.

4.1 Results

By using the collapsed input data set, the problem became stable enough to find a solution and form predictions of the output data. The predictions, shown in Figure 4.1, have RMSPE values of 3.51%, 4.32%, and 8.55% for the burnup, enrichment, and cooling time, respectively. The burnup predictions are all within 6 GWd/MTU, the enrichment predictions are all within 0.5% U-235, and the cooling time predictions are all within 2.5 years of their respective actual values. These errors are lower than expected, based on how the input data meets the

assumptions of the model. The burnup has the lowest RMSPE of the three outputs, which supports that it has the most linear relationship to the radiation signatures. The cooling time has the highest error of the three outputs, which is consistent with it having a nonlinear relationship with the input. When the actual and predicted are compared, the burnup and enrichment predictions appear to only have random noise on either side of the actual value. The cooling time predictions show random noise around the actual value until values of 20 years, at which point biases are introduced. The highest cooling time, 30 years, is always under predicted while values of 20 and 25 years are always over predicted. The burnup and enrichment predictions meet the accuracy requirement, as their RMSPE values are less than 5%. The cooling time predictions do not meet the requirement well, because 41.7% of the predictions are more than $\pm$ 1 year from the actual value.

Even though this model meets some of the prediction requirements and shows promising results, the condition number is 9.35×10^{37}. This value is well above the applied threshold of 100 for this work and therefore this is not a stable model. Although the relatively low prediction error of the model, below 10%, may suggest that the system is more linear than initially anticipated, the instability of the model reduces the likelihood of this observation being true.

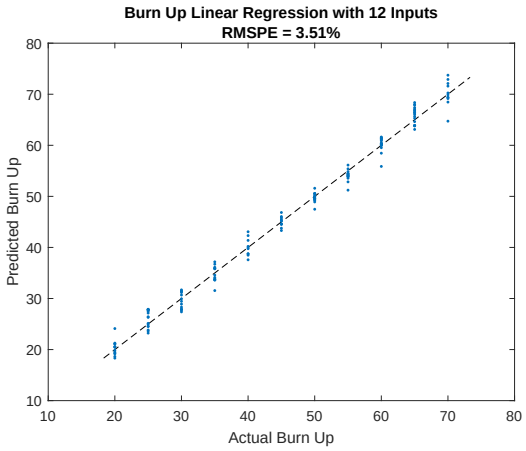

(a) Predicted vs actual values of burnup.

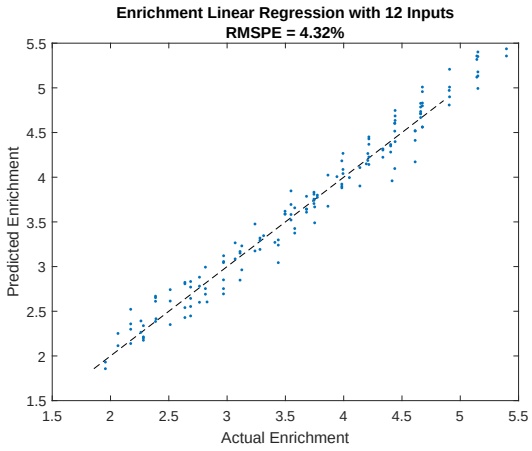

(b) Predicted vs actual values of enrichment.

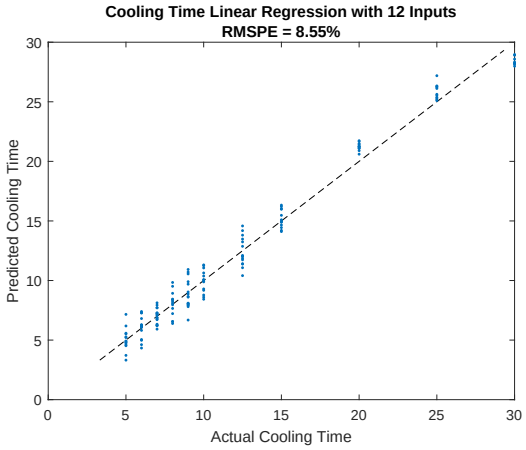

(c) Predicted vs actual values of cooling time.

Figure 4.1: Ordinary Least Squares Regression prediction results as a function of the actual value, using the collapsed testing data set.

Chapter 5

Principal Component Regression

The next modeling technique used is Principal Component Regression (PCR). This method is based on a linear transformation of the input data, X, by multiplying it by a loading vector, p_i, to result in the Principal Component (PC) scores, t_i [25]. This matrix multiplication is shown in Eq. 5.1.

$$t_i = X * p_i \tag{5.1}$$

The loading vectors to perform this transformation are the eigenvectors of the covariance matrix of the input data. The resulting PCs are constructed to maximize the amount of variance contained in each PC while being constrained to be orthogonal to each of the previous PCs. An example of this is shown in Figure 5.1, in which the first PC is in the direction of the largest variance of the data, and the second PC is in the direction of the next largest amount of variance while orthogonal to the first PC. The intersection of each of these directions creates the new coordinate system for the data in the PC space. The orthogonality constraint ensures that the transformed data is not correlated.

The PCs can be analyzed in a variety of ways to glean more information about the data, often referred to as Principal Component Analysis (PCA). Viewing the PC scores with respect to each PC can identify underlying trends in the data, such as nonlinearities from specific variables. This has been performed on a similar data set to what is used in this work by Hellesen et al. [23] to investigate the degree of linearity of different fuel characteristics. They found that the cooling time has a very nonlinear relationship with the first 3 PCs of their

input data, while the burnup and enrichment are linear with respect to the first 2 PCs and are nearly orthogonal to each other. Since the PCs are ordered by the amount of variance they explain of the original data, PCA is often used for denoising data sets by removing PCs that do not contain significant information about the system. Denoising can be done in a variety of ways, including applying a threshold on the percentage of the variance of the input data to explained, comparing the eigenvalues of each PC, or any other dimensionality reduction method. Once the noisy PCs are removed, the selected PCs are transformed back to the original data space by manipulating Eq. 5.1. Data in the PC space can also be used to calculate statistics about the variation within and outside of a given model, the T^2 and Q statistics respectively, which allow PCA to be used for process monitoring [30, 38].

In addition to analysis, the PCs can be used to calculate regression coefficients to relate this input data to the desired outputs, which is referred to as Principal Component Regression (PCR). For this work, only linear regression is used with this transformation, although many techniques can be used to perform the regression, such as non-parametric techniques [21]. The use of OLS for regression means that PCR is subject to the same assumptions as OLS. However, since the input data in PCR is all orthogonal and uncorrelated, it is expected that assumption 4, that the inputs are all independent, is better met using this technique. This leads to the expectation that PCR models are more stable than those using OLS and a very useful tool for highly correlated input data. Due to PCR being a dimensionality reduction technique, not all of the PCs calculated should be used to perform the regression. There are a variety of methods to determine how many PCs should be kept, based on balancing the simplicity of the model and the loss of information from the PCs not used. Each of the methods must be compared for how they impact the prediction accuracy, stability, and simplicity of the model.

In this work, PCA will be performed on the data set, with the scores of the first 3 PCs visually analyzed to identify trends of the data in the PC space. Then five different PCR models will be built using different methods to determine the number of PCs to use: the amount of variance that each PC explains, the eigenvalues of the PCs, the correlation of the PCs to the output, Akaike Information Criteria (AIC), and cross validation of testing and training error.

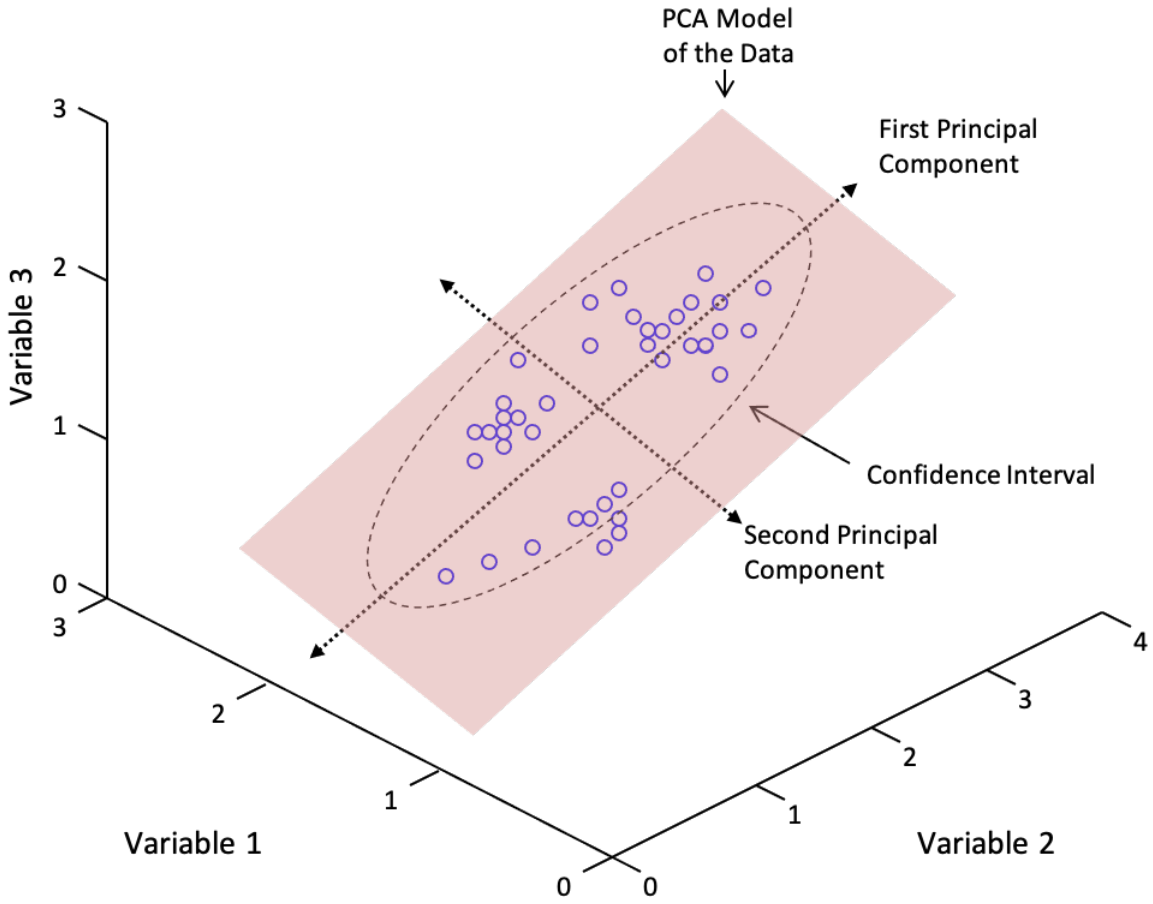

Figure 5.1: Visual example of the resulting PC scores. The PCs shown are all orthogonal, while capturing the largest amount of variance possible. Figure provided by J. B. Coble.

5.1 PCA

The PC scores of the training data were examined for the first three PCs. This data set was chosen, as opposed to the entire emissions data set, because it is what is used in the regression step of PCR. When the first and second PC are compared, Figure 5.2, there is a clear nonlinear relationship between these PCs. When the scores are organized by their burnup, Figure 5.2a shows that as the burnup increases, the relationship with these PCs becomes more nonlinear until a maximum is reached around 65 GWD/MTU. The nonlinearity between these PCs seems to mostly fit a quadratic relationship except a small concave up section around a PC 1 value of -20. The width of the concave down curve and spread of the scores increases with burnup as well. Looking at the loadings of these PCs, to discover why these PCs would have this relationship, the first PC has approximately even loadings for each of the energy bins meaning that each energy bin has similar contributions to the scores of the data in the PC space. The second PC shows a strong loading from the energy bin corresponding to the 662 keV peak from Cs-137 decay and negative loading from the energy bins corresponding to a 1.506 MeV peak.

An opposite trend is observed when the scores are grouped by their cooling time. Figure 5.2b shows that as the cooling time increases, the scores become more linear and the observations become more clustered together. The nonlinearity between these PCs with respect to the cooling time appears to be more sinusoidal than quadratic, but completely disappears around a cooling time of 20 years, when it becomes a linearly decreasing cluster. These patterns of these two variables appear to have a perpendicular relationship, based on the direction of scores as each variable is increased. This relationship is to be expected based on the orthogonality of the PCs if these variables are independent, which is confirmed by a correlation coefficient of 0 between these two variables. Finally, Figure 5.2c shows that when the scores are organized by enrichment, with the burnup of each observation indicated by the shape of the marker, there is no unique pattern observed. In this figure, each enrichment value appears to represent a subset of the clusters of scores based on burnup, with only one enrichment value per small cluster along the burnup trend lines. This indicates that the enrichment impacts the exact values of the scores, but the burnup has a larger impact on the shape of trend line of the scores. The connection between these two variables and the lack of unique trends for the enrichment are not surprising, given that the enrichment values are based on the burnup.

When the first and third PC as examined, Figure 5.3, similar nonlinearities are observed. When grouped by burnup, Figure 5.3a shows that all values of burnup have a nonlinear behavior between these PCs with the width of the curve increasing with burnup, similar to the trend with respect to the second PC. The value of the third PC also decreases as the burnup value increases, indicating a negative correlation between this PC and the burnup. The third PC has a strong negative loading from the energy bin containing the 662 keV decay of Cs-137 and a strong positive loading from the energy bin of the 1274 keV peak from the decay of Eu-154. Eu-154 is known to have a quadratic relationship to burnup, which would influence the nonlinear relationship between the burnup and third PC. When the scores are grouped by their cooling time, Figure 5.3b shows that there is an opposite pattern to what is observed in the burnup groupings; there is increased linearity and decreased peak width as the cooling time increases. The opposite direction of these trends supports the lack of correlation between the burnup and cooling time observed by the first and second PC. The clustering of the scores for each cooling time also becomes wider as the cooling time increases. Finally, when the scores are grouped by their enrichment, Figure 5.3c shows that there is still no unique trend and is very similar to what is observed from the first and second PC. The enrichment values follow the existing trend of the burnup, with no small clusters along those trend lines. Overall, the trends observed from these PCs are similar to what is observed between the first and second PC, but with some changes in the direction of the trends.

Based on the information in these figures, the third PC has the most linear relationship between the burnup and initial enrichment of the fuel. This is due to the most even spacing between observations with respect to this PC. This is not a perfectly linear relationship, but it is stronger than that of the characteristics and the first and second PC. This is confirmed by correlation coefficients of -0.7011 and -0.6456 between the third PC and the burnup and enrichment, respectively. The negative sign of these values indicates that it is a negative correlation between the variables, as suggested by the observations of Figure 5.3a. The cooling time appears to have the most linear relationship with the first PC, based on the spacing of the observations with respect to these variables. The correlation coefficient between these variables is 0.597, which indicates less of a linear relationship between these variables and the relationship between the burnup or enrichment and the third PC. However, the cooling time and first PC still have some linear correlation. Since the first PC has fairly even loadings for all energy bins and the entirety of the spectrum will decrease with time, it is unsurprising that this PC is most correlated to the cooling time. It is not a perfectly

linear relationship because of exponential decay relationship between emission intensity and time.

When the first three PCs of a similar, but smaller, input data set were examined [23], similar nonlinearities with respect to the cooling time were found. However, there was a linear relationship with respect to the burnup and enrichment that was not observed with this data set. The changes with respect to the enrichment are due to the use of enrichment values independent of the burnup, which would remove the consistency in the trends of these variables in this data set. The analysis previously done suggests that the nonlinear relationship observed will lead to large errors in predicting the output data, based on assumption 1 of OLS. Based on this suggestion, low cooling times and burnup values would be expected to have the lowest prediction error, since these groups have the most linear relationship with the first three PCs. It was also observed by Hellesen et al. that when the cooling time is held constant and the scores are organized by their burnup and enrichment, that these two variables have perpendicular trends. This was not observed in this data set, with the opposite being observed; the burnup and enrichment have a colinear trend due to their correlation.

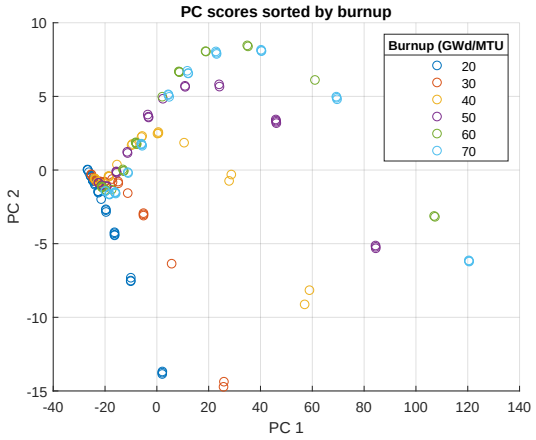

(a) PC Scores organized by burnup

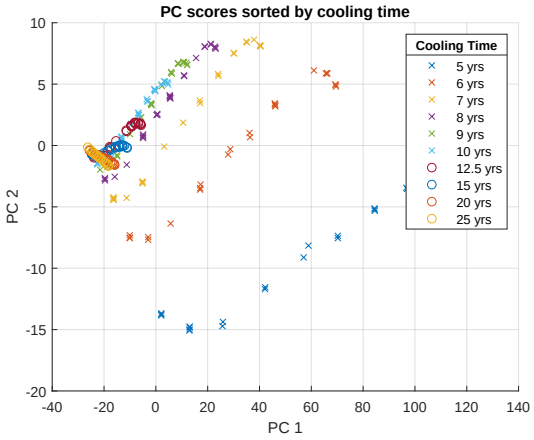

(b) PC Scores organized by cooling time.

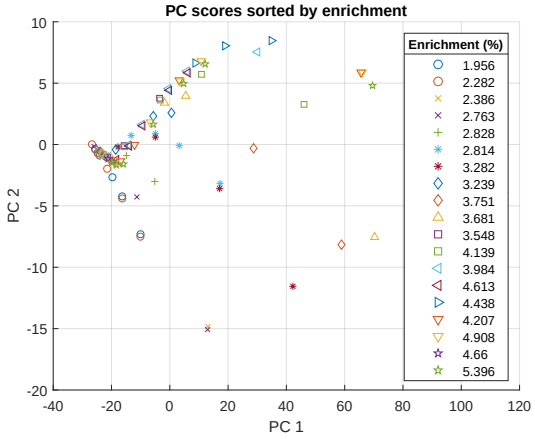

(c) PC Scores organized by enrichment.

Figure 5.2: Input PCA scores of the first and second PC.

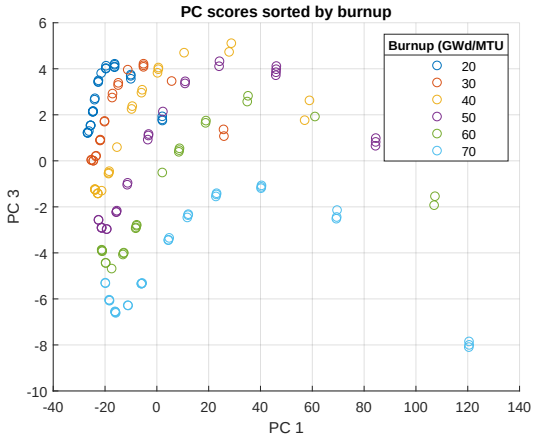

(a) PCs organized by burnup.

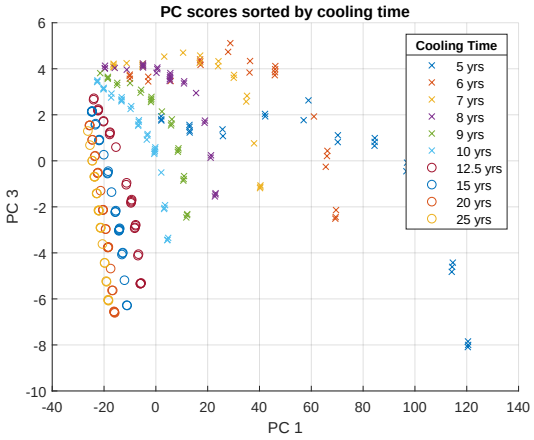

(b) PCs organized by cooling time.

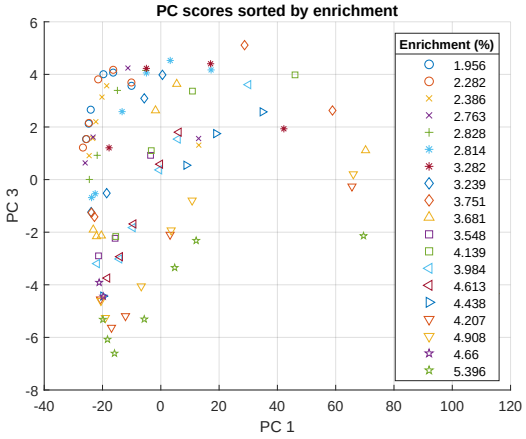

(c) PCs organized by enrichment.

Figure 5.3: Input PCA scores of the first and third PC.

5.2 Amount of Variance

The first method to determine the number of PCs is the amount of variance that is cumulatively explained by the addition of each PC. The amount of variance that each PC explains can be calculated as the eigenvalue of the PC divided by the sum of the eigenvalues for all PCs, with the cumulative variance using the sum of all PCs used in the numerator. A threshold can be applied to the cumulative amount of information explained by each set of PCs to determine how many PCs should be used. The PCs that are not used are then considered to be noise and are not used. For this work, a threshold of 95% of the variance was used.

The threshold is reached by using only the first PC, which explains 96.43% of the variance of the original data. The high percentage of the variance explained by just this PC supports that the input data is highly correlated. When only the first PC is used to perform PCR and predict the output data, the predictions have a much higher error than the OLS model, as shown in Figure 5.4. The predictions for burnup, enrichment, and cooling time have RMSPE values of 31.26%, 21.96%, and 48.36%, respectively. The predicted burnup values vary in their accuracy to the actual value, with some predictions accurate to within 10 GWd/MTU of the actual value and other predictions accurate to within 30 GWd/MTU. The enrichment predictions for this model have a greater range of error than the OLS model, with some predictions more than 1.5% U-235 from the actual value. The cooling time predictions are over 13 years away from the actual value.

Each set of predictions contains a significant bias. The predicted burnup values do not go below 40 GWd/MTU, predicted enrichment values do not go below 3.4%, and the predicted cooling times do not go above 18 years. The model also predicts negative values for the lowest cooling times, which strengthens the bias of under predicting this characteristic. It is not surprising that burnup and the enrichment show a similar bias, since they are correlated. The predictions of each variable appear different from what would be expected based on PCA. The lower burnup values and higher cooling time values appear to have the most linear relationship with respect to the first PC but are never accurately predicted. When the errors of the predictions are examined as a function of the variable being predicted, shown in Figure 5.5, an opposite effect is shown. The lower burnup and higher cooling times have the highest average error of prediction, but they also have the smallest range of prediction error. This means that these observations have the lowest prediction variances, but the highest bias. A similar effect is observed in the enrichment predictions as the burnup

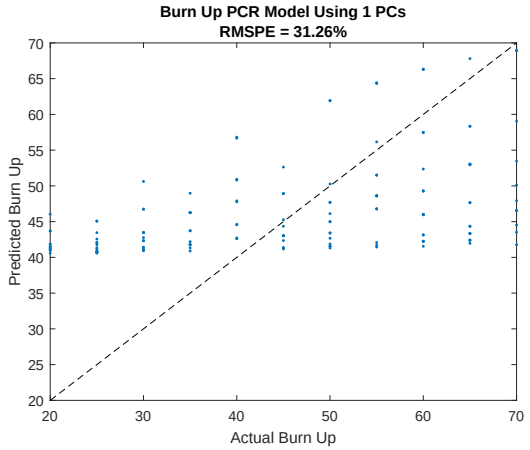

(a) Predicted vs actual values of burnup.

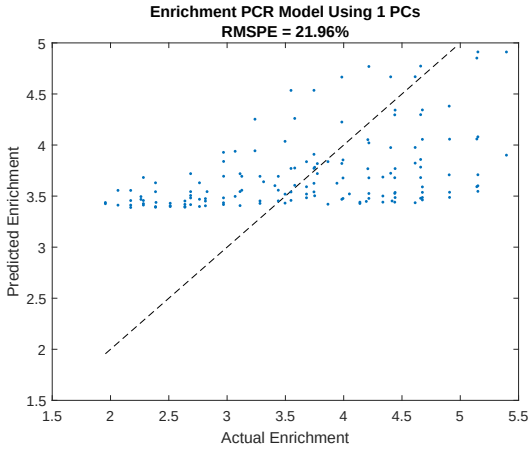

(b) Predicted vs actual values of enrichment.

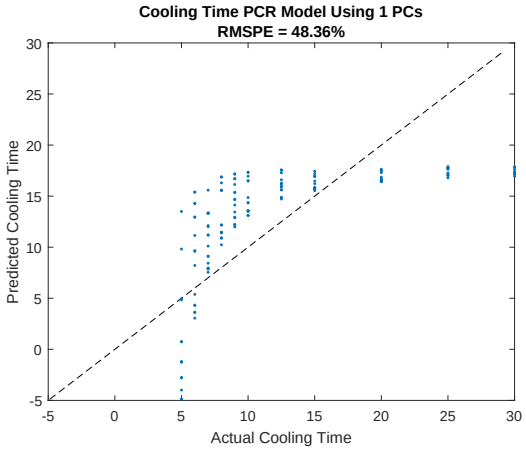

(c) Predicted vs actual values of cooling time.

Figure 5.4: Comparison of actual and predictions for PCR model built with 1 PC.

predictions. Figure 5.5b shows some very nonlinear behavior in error as a function of the cooling time, which suggests that there is some nonlinear behavior in the system that is not being captured by the model.

None of the predictions of this model meet the accuracy requirements. The burnup and enrichment RMSPE values are both above 5%, and 90.7% of the cooling time predictions are more than 1 year away from the actual value. The results from this model shows that

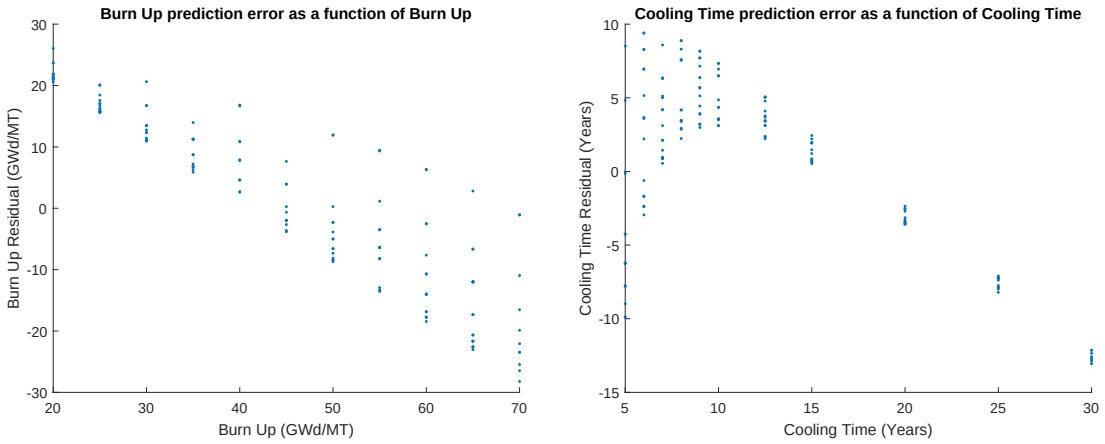

(a) Burnup prediction error as a function of burnup.

(b) Cooling time prediction as a function of cooling time.

Figure 5.5: Prediction error as a function of the variable predicted

despite most of the input data being highly correlated in a similar way, the information in other directions is relevant to the outputs. To provide an accurate prediction of the outputs, additional PCs will be required.

Despite the poor prediction results of this model, the use of only 1 PC means that the model has a condition number of 1. This means that the model is stable and will consistently produce almost the same results. Therefore, the biases in the predictions will always be present using this model.

5.3 Eigenvalues

The next method is based the eigenvalues of the PCs, and is often referred to as the Kaiser Criterion [39]. It is a general principle for various forms of factor analysis that suggests the use of factors with latent roots greater than the roots of the correlation matrix. When applied to PCR, the latent roots used are the eigenvalues and the roots of the correlation matrix is 1, since the data is standardized. It can also be thought of in terms of the distribution of the information to each PC. The eigenvalue of each PC is correlated to the information

it contains and the sum of all of the eigenvalues is the number of PCs calculated. If all of the information of the input data were distributed equally amongst the PCs, then each eigenvalue would be 1. Therefore, it can be assumed that a PC with an eigenvalue greater than 1 would contain more information than the amount expected to be contained in the PC. The selection of PCs with an eigenvalue greater than 1 can remove PCs that contain less information that what they are expected to contain and can be considered noise.

Figure 5.6 shows the eigenvalues of the first 20 PCs on a semi-log scale, with the red dashed line at 1 to provide a reference of when the eigenvalues go below 1. From this figure, it is observed that the eigenvalue of PC 5 is below 1 (exact value is 0.4095), which results in the use of the first 4 PCs for these models. These PCs are able to explain 99.94% of the variance of the original data. This model uses three more PCs than the previous model, which indicates that although these additional PCs are not able to explain a large portion of the variance, they are still potentially valuable information about the output space.

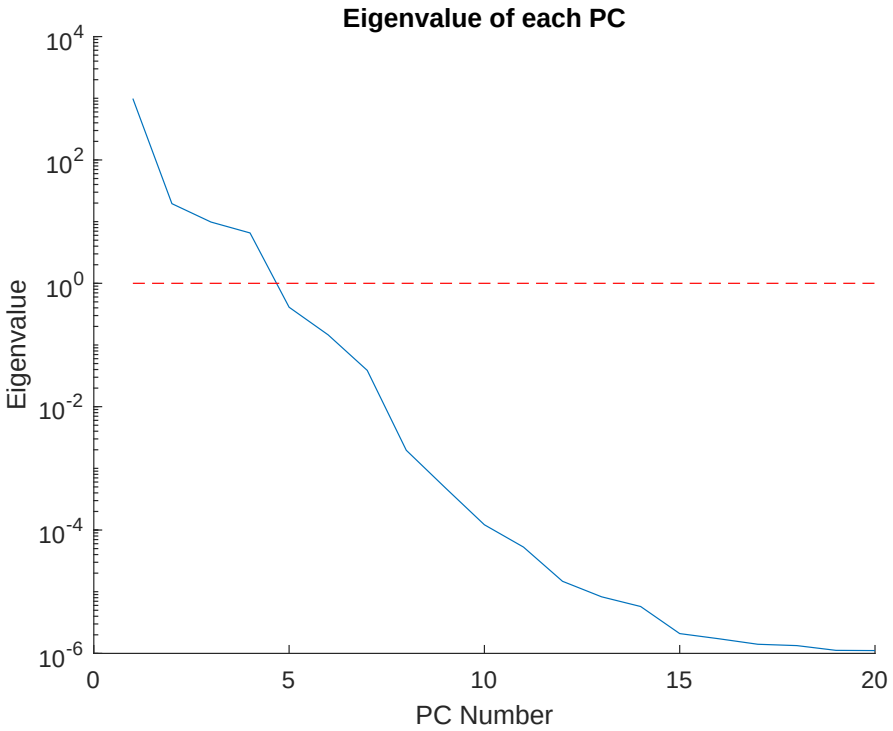

Figure 5.6: Eigenvalues of the first 20 PCs.

By using the first 4 PCs the predictions for this model, shown in Figure 5.7, have a much lower percent error than the previous PCR model. The burnup, enrichment, and cooling time RMSPE values are 7.45%, 8.23%, and 20.48%, respectively. All of the predictions are within 15 GWd/MTU, 1% U-235, and 8 years for the burnup, enrichment, and cooling time, respectively. The range of error in these predictions is about half the range for the errors of the previous model.

The improvement in the RMSPE values and range of prediction error suggests that the three additional PCs, while not able to explain a significant amount of information about the input data, are able to explain more information about the output data. None of the predictions appear to have the extreme biases present in the previous model, but there are still some present. In the burnup predictions, the lowest and highest values are consistently over predicted, in the enrichment predictions only the lowest values are consistently over predicted, and in the cooling time predictions values of 10-20 years are over predicted while values of 30 years are under predicted. While these are much less severe than the biases of the previous model, they do indicate that additional information about the output data is required to remove these biases. Despite the improvement in prediction accuracy, the results of these models also do not meet the prediction requirements. The burnup and enrichment RMSPE values are above 5%, and 70.9% of the cooling time predictions are more than 1 year from the actual value.

The improved prediction performance of this model comes at the expense of the use of three additional PCs, compared to the previous model. This results in the increase of the condition number to 150.8. Although this is the lowest condition number of any model thus far, it still higher than what is considered stable.

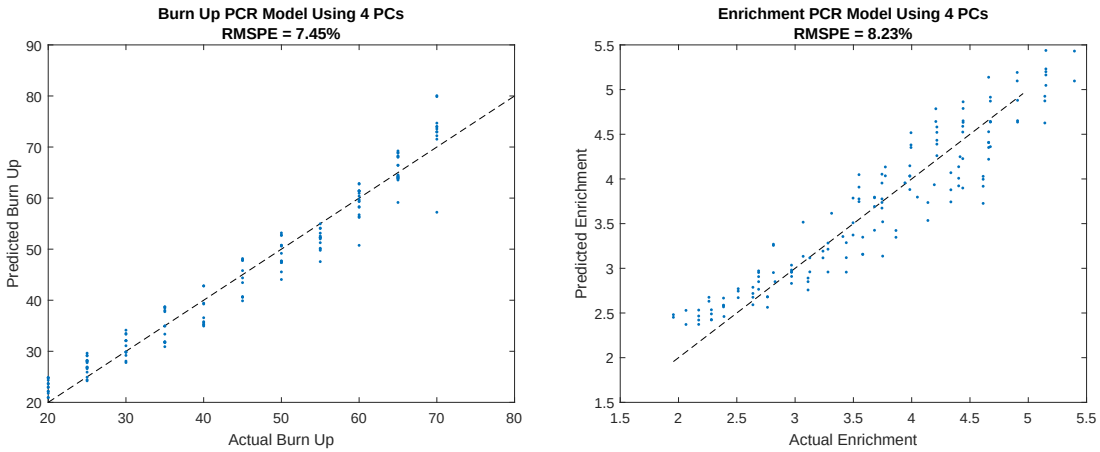

(a) Predicted vs actual values of burnup. (b) Predicted vs actual values of enrichment.

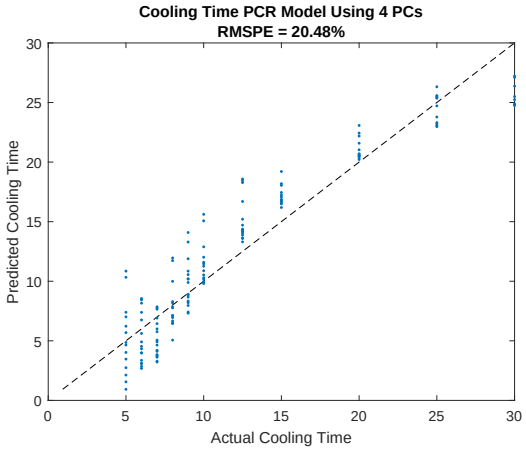

(c) Predicted vs actual values of cooling time.

Figure 5.7: Comparison of actual and predictions for PCR model based on eigenvalues.

5.4 Correlation to Output

The third set of models built using PCR considers the correlation of each PC to each of the output variables. For this work, a correlation coefficient of 0.6 was used to determine which PCs to use. This resulted in using only the third PC to predict the burnup and enrichment, and zero PCs were used to predict the cooling time. Based on Figure 5.3, it is not surprising

that the third PC is highly correlated to the burnup and enrichment, but it is surprising that the first PC is not well correlated to the cooling time. Upon further inspection, the correlation coefficient between the first PC and the cooling time is -0.597. While this is less than the specified threshold, it still shows a relatively strong linear relationship that should be considered in this model. For this reason, the correlation threshold was lowered to 0.575. This did not change the PCs that are used for the burnup and enrichment predictions, but it did add PC 1 to the model to predict the cooling time.

When these PCs are used to predict each of the outputs, the RMSPE values for the burnup, enrichment, and cooling time predictions are 26.59%, 19.16%, and 48.36%, respectively, as shown in Figure 5.8. The errors in each of the predictions are within 25 GWd/MTU, 2% U-235, and 14 years for the burnup, enrichment, and cooling time, respectively. Overall, these models perform much worse than the ones based on the PC eigenvalues, but the burnup and enrichment prediction RMSPE values are slightly lower than the PCR models based on explaining 95% of the input data variance. The burnup and enrichment predictions have some bias; the lowest values are over predicted, and the higher values are under predicted. The predictions of the cooling time are exactly the same as the output of the model based on explaining 95% of the variance of the input data. These models also do not meet the requirement, as the burnup and enrichment predictions are above 5%, and 90.7% of the cooling time predictions are more than 1 year from the actual value.

The condition number of each of these models is 1 since they each use only one PC and are thus considered stable.

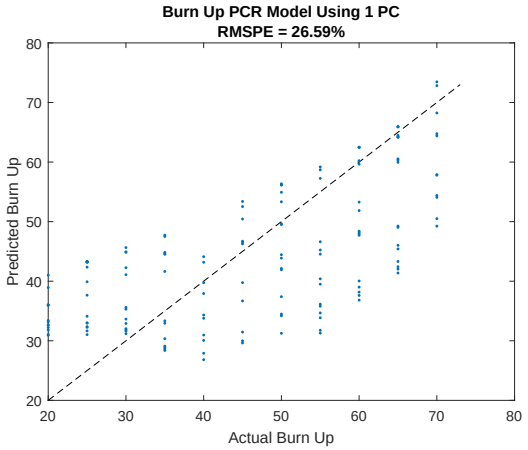

(a) Predicted vs actual values of burnup.

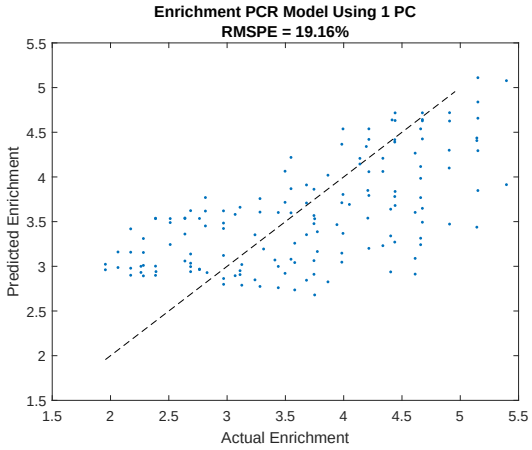

(b) Predicted vs actual values of enrichment.

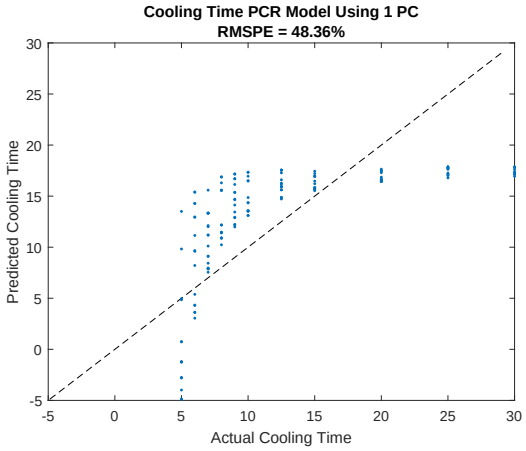

(c) Predicted vs actual values of cooling time.

Figure 5.8: Comparison of actual and predictions for PCR model built with PCs correlated to the output.

5.5 Akaike Information Criteria PCR

The fourth set of models uses AIC to determine the number of PCs to use, which is described in Section 2.3.1. Since the PCR transformation is only dependent on the input data, the AIC value is also only a function of the input data and leads to the same number of PCs to predict

each output. The calculated AIC value as a function of the number of PCs used is shown in Figure 5.9. This figure shows that with the addition of each PC, the AIC value decreases, until the maximum number of PCs, 302, is used. However, this figure can be treated as a scree plot due to the clear change in slope. By taking this approach, the minimal decrease in the AIC value after the bend in the curve can be seen as not significant enough to warrant the use of the additional PCs, and the bend in the curve is the appropriate number of PCs to use. This bend is estimated to occur at 14 PCs.

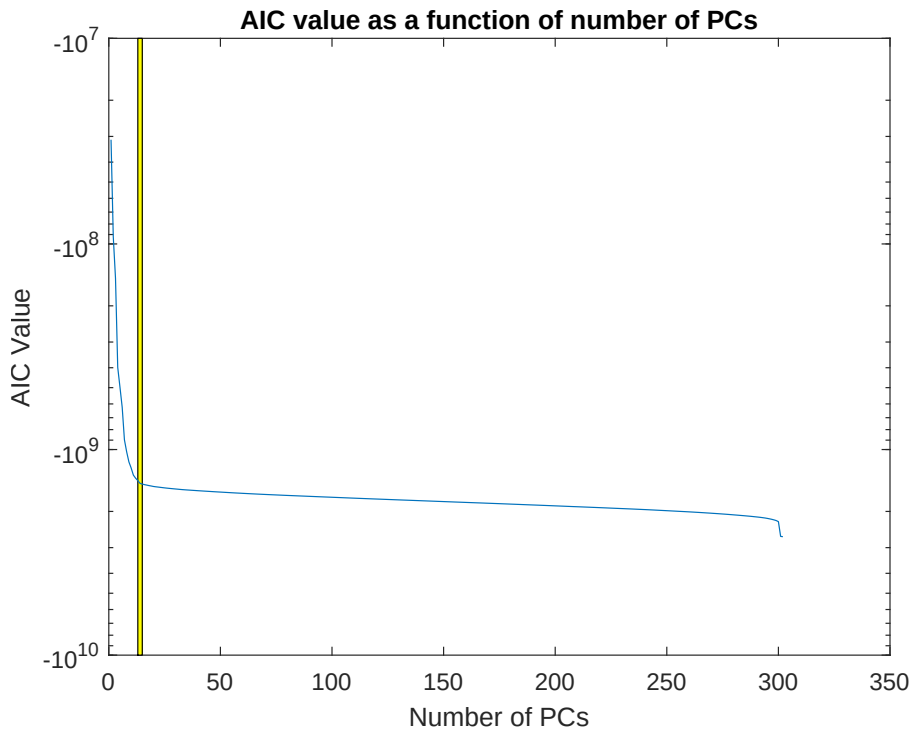

Figure 5.9: AIC of the testing data as a function of number of PCs. The highlighting shows the location of 14 PCs.

These models exhibit the best prediction performance of any of the PCR models built thus far. As Figure 5.10 shows the predictions for burnup, enrichment, and cooling time have RMSPE values of 0.61%, 1.78%, and 5.24%, respectfully. The predictions are all within 1.5 GWd/MTU, 0.25% U-235, and 2 years of the actual values of burnup, enrichment, and cooling time, respectively. These predictions contain almost no consistent bias, unlike many of the previous models. The burnup predictions have fairly consistent predication

variances for each value of burnup, while the enrichment predictions show an increase in the prediction variance with an increase in the value of enrichment. This is most likely due to the increased variation in the enrichment values that is not present in the burnup values. since the noise is a consistent percent, the absolute noise increases as the enrichment increases. The larger absolute noise would contribute to a larger prediction variance. The cooling time predictions do not have a similar trend in the prediction variance. The only notable aspect of the predictions is that a cooling time of 20 years is always over predicted. The burnup and enrichment meet the accuracy requirement since both of their RMSPE values are below 5%. For the cooling time predictions, 6.62% of the predictions are more than 1 year away from their actual value. While not all predictions meet the requirement, this model has the lowest percentage of observations outside the interval. This model has a condition number of 1.7176×10^8, due to the last smallest PC used having an eigenvalue on the order of 1×10^{-6}. The large condition number of this model means that it is unstable.

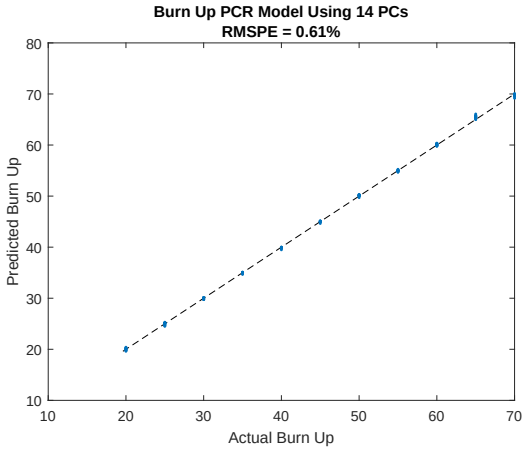

(a) Predicted vs actual values of burnup.

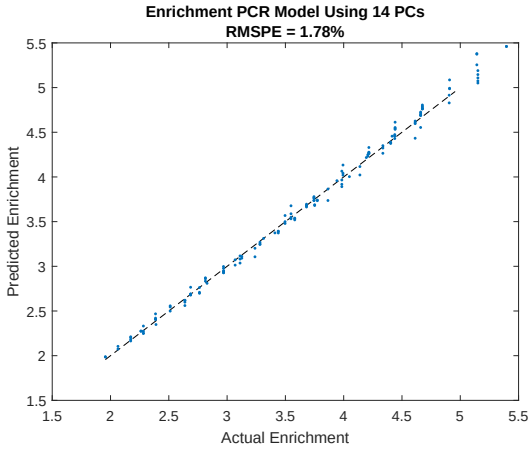

(b) Predicted vs actual values of enrichment.

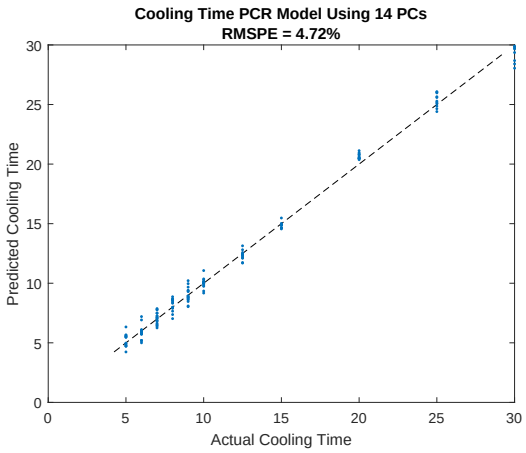

(c) Predicted vs actual values of cooling time.

Figure 5.10: Comparison of actual and predictions for PCR model based on AIC.

5.6 Cross Validation

The final set of PCR models were constructed based on cross validation, which is described in Section 2.3.1. An upper limit of 20 was placed on the number of PCs that could be used for these models based on observations of the results of the previous PCR models constructed and the characteristics of the 20th PC. The first 20 PCs explain almost 100% of the original

data, and the eigenvalue of the 20th PC is 1.111×10^{-6}, so it can be assumed that any PCs beyond 20 will only contribute noise to the predictions, decrease the stability of the model, and increase the chance of overfitting the model. Therefore, when performing cross validation, only the RMSPE of models using 20 PCs or less are considered.

Figure 5.11 shows the RMSPE of each output predictions using the testing data set as a function of the number of PCs used. The lowest RMSPE values are shown by the magenta circles on this figure and occur at 17, 19, and 14 PCs to predict the burnup, enrichment, and cooling time, respectively. Both cross validation and AIC lead to the use of 14 PCs to predict the cooling time. This consistency suggests that this is the true dimensionality in the PC space.

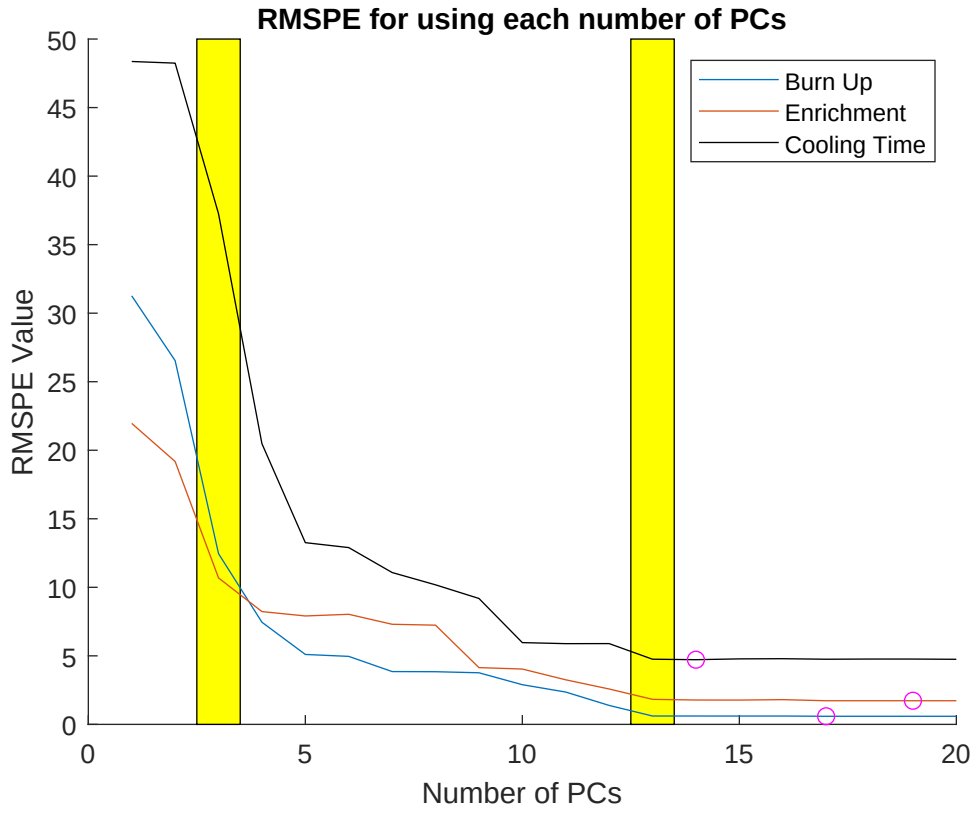

Figure 5.11: RMSPE of the testing data predictions for each output as a function of number of PCs.

When these models are used to predict the testing data, as shown in Figure 5.12, the error is much lower than the previously built models, which is to be expected. The RMSPE values for the burnup, enrichment, and cooling time predictions are 0.59%, 1.72%, and 5.24%, respectively. The predictions are all within 1 GWd/MTU, 0.2% U-235, and 2 years of the actual values of burnup, enrichment, and cooling time, respectively. In the burnup predictions, there is a bias of over predicting values of 65 GWd/MTU, and 70 GWd/MTU predictions have the highest prediction variances, which both indicate that the performance degrades at higher burnup values. However, they are still accurate within 1 GWd/MTU, so it may not be a large concern since that is still a very low prediction error. The enrichment predictions yet again show an increased prediction variance as the value of enrichment increases, but the errors are within 0.2% U-235 which is very low. The predictions of the cooling time are exactly the same as the previous model since they use the exact same PCs. The burnup and enrichment predictions of these models meets the accuracy requirements because they both have RMSPE values less than 5%. The cooling time results 6.62% of the predictions are more than 1 year away from the actual value, same as the AIC PCR model.

However, when the condition number of each model is examined, they greatly exceed the threshold: 7.03×10^8, 8.83×10^8 and 1.72×10^8 for each model, respectively. Therefore, despite the great performance in prediction accuracy, these models are also unstable.

It is observed in Figure 5.11 that each of the curves appears to reach a constant error at 13 PCs, shown by the right highlighted section in Figure 5.11. Based on intuition, it may be suggested to use 13 PCs instead to create a simpler, more stable model despite the known increase in prediction error. However, when the condition number for such a model was calculated, it is 1.20×10^8, which means that this would also be an unstable model, even if the increase in error is minimal. Based on Eq. 3.4, using at most the first 3 PCs would result in a stable condition number (100.43), which would be expected to have relatively poor prediction performance based on left highlighted section of Figure 5.11, at 10-35% RMSPE. This shows the exaggerated trade-off between stability and prediction performance when using PCR for highly correlated data.

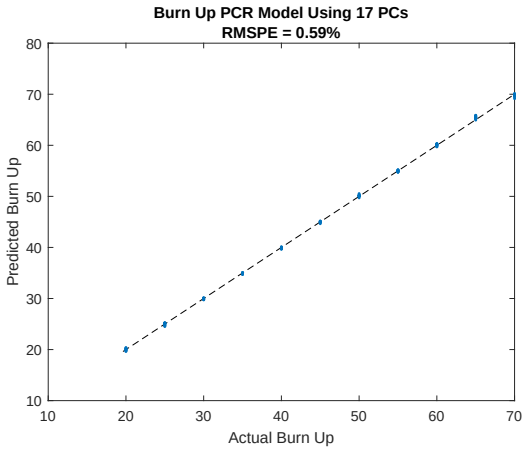

(a) Predicted vs actual values of burnup.

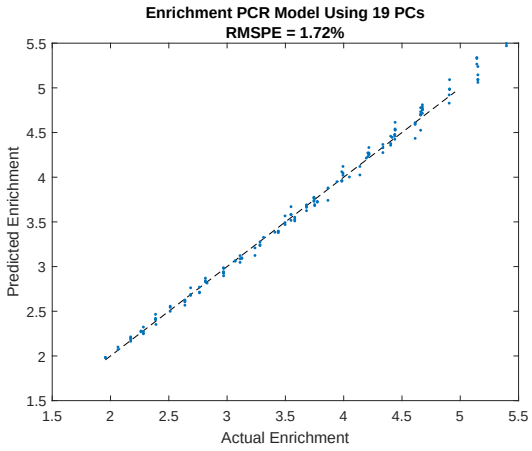

(b) Predicted vs actual values of enrichment.

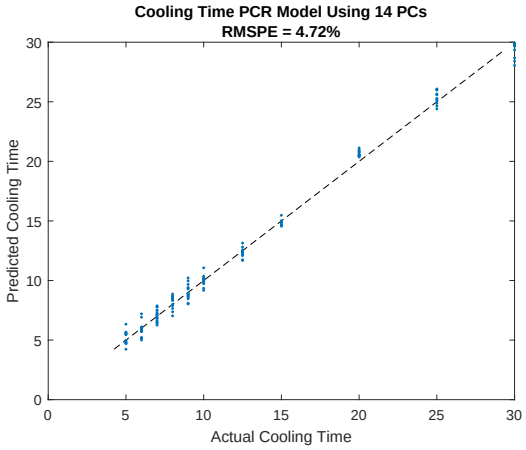

(c) Predicted vs actual values of cooling time.

Figure 5.12: Comparison of actual and predictions for PCR model built with PCs based on cross validation.

Chapter 6

Partial Least Squares Regression

The final modeling technique used in this work is Partial Least Squares Regression (PLS). PLS utilizes a linear transformation on the input and the output data into a latent variable (LV) space in which multilinear regression is performed. The entire process is performed through two different linear transformations: an outer transformation and an inner transformation. The outer transformation is used to transform the inputs and outputs into the LV space such that each of the latent variables explains a maximized amount of the correlation between the input and output space. In contrast to the PCR transformation, the scores of the observations are multiplied by the loading vectors and added to any residuals to result in the original data, as shown in Eqs. 6.1 and 6.2.

$$X = t_i * p_i + E_i \tag{6.1}$$

$$Y = u_i * q_i + F_i \tag{6.2}$$

In these equations, q_i and p_i are the loadings for output and input latent variables, and u_i and t_i are the score vectors of the observations in the LV space. The scores, similar to PCR, are ordered by decreasing amount of the covariance between the input and output data. The outer transformation collapses correlated information into the same scores, so that each of the loadings of the input and output are not correlated.

The inner transformation performs a specified type of regression between the scores of the input and output variables. Traditionally, a linear regression is used to perform this

transformation, as shown in Eq. 6.3. This is used to define a relationship between the input and output in the LV space.

$$u_i = b_i * t_i + \epsilon_i \tag{6.3}$$

This transformation still contains the same assumptions described in Chapter 4, however the outer transformation helps to ensure that the inner transformation performs a single input, single output regression. Therefore, there is no concern of the input variable being correlated with other input data, although it is still correlated to the output data. Based on this, assumption 4 of OLS is met.

Although the outer transformation helps to ensure that assumptions 4 and 5 of OLS are better met, it does not guarantee that assumption 1 is met when using PLS; the system may not be linear in the LV space. For these systems, the PLS algorithm can be adapted to contain a nonlinear regression as the inner transformation. Multiple methods have been explored and used in place of a linear inner transformation, such as splines [40], neural networks [41], and k-nearest neighbors [7]. To determine if the inner transformation should be nonlinear, the input and output scores for the first few LV can be plotted and visually inspected for a nonlinear relationship. The presence of identifiable nonlinearities will suggest that another form of regression should be used in place of OLS.

The PLS transformations can be calculated through a variety of algorithms, with the SIMPLS [42] and simplified PLS algorithms [37] being employed in this work. Both algorithms require the use of standardized input and output data. The SIMPLS algorithm is based on the singular value decomposition of the cross product of X^TY, with the weights used to calculate the scores as the first left singular vector. The loadings are then calculated using a pseudoinverse of the scores with the original data, and the regression coefficients are calculated as the difference between the weights multiplied by the scores and the original output data. The simplified PLS algorithm constrains the projections of $X * u_i$ to be orthogonal while maximizing $(u_i^T X^T y)^2$ [37]. This optimization is based on this quantity equaling the square of the correlation between the projections and the product of the outputs and variance of the projections. This algorithm also requires iterative calculations for each set of LV scores and loadings but does not require iterations for the convergence of the loadings. Both of these methods constrain the projections to be orthogonal to the previous LVs, although this is not a constraint of all PLS algorithms. To predict the output of a new set of data, it must be transformed into the LV space using the same algorithm that

was used on the training data set. The regression coefficients in b are then used to make a prediction of the output in the LV space, which are then transformed to the original data space and unstandardized.

PLS has been used for a variety of chemometrics modeling [43, 44]. In these systems, PLS has been shown to have better stability than OLS, a lower predicted sums of squares than OLS and PCR [43], and can often use fewer components than PCR to achieve the minimum error. As a dimensionality reduction tool, it has been shown to have improved performance over PCR when additional noise elements are added to the data [37]. These previous results suggest that PLS should have the best performance in terms of stability, parsimony, and prediction results.

When using PLS, similar to PCR, some LVs can be considered noise in the system and there are a variety of ways to determine the number of LVs that should be used. For this technique, two primary methods will be applied to build four different models. The first model predicts all of the outputs in a multilinear regression, and uses LVs informed by cross validation. This model is based on PLS being a supervised transformation, suggesting that it will have different performance from models to predict a single output. The next set of models will each predict a single output and uses LVs informed by AIC. The third set of models will be constructed based on a PLS transformation of a single output, and the fourth model will use a nonlinear inner transformation and predict only the cooling time. These last two models use cross validation to inform the number of LVs to use. The last model is based on the relationship of the input and output scores of the first LV from the third set of models. Each of these models is built using the SIMPLS algorithm, except the nonlinear model, which is built using the simplified PLS algorithm. This is due to the ease of reconstructing this model to provide the necessary adaptation of the inner transformation. These algorithms have been shown to provide the same results when used with a single output variable [42], so there is no concern over accuracy differences in the use of a different algorithm.

6.1 Multilinear Regression Model

This first PLS model was built to test the performance of a multilinear regression model. Cross validation of the testing RMSPE was used to determine the number of LVs to use for this model. Since all outputs are predicted in the same model, the number of latent variables used cannot be tailored for each output, like they were for the PCR models built. Therefore,

the cross validation is performed using an averaged error of the outputs as a function of the number of LVs used. The highlighted section of Figure 6.1a shows the minimum RMSPE value occurring around 15 LVs. When this plot is zoomed in to only compare the errors of models using up to the first 20 LVs, Figure 6.1b, the lowest RMSPE value does occur at 15 LVs, indicated by the magenta circle. However, the error begins to flatten at 13 LVs, shown by the highlighted section of this figure. Since there is no visible difference between the error and either model is expected to be stable, the 13 LV model was chosen due to its simplicity.

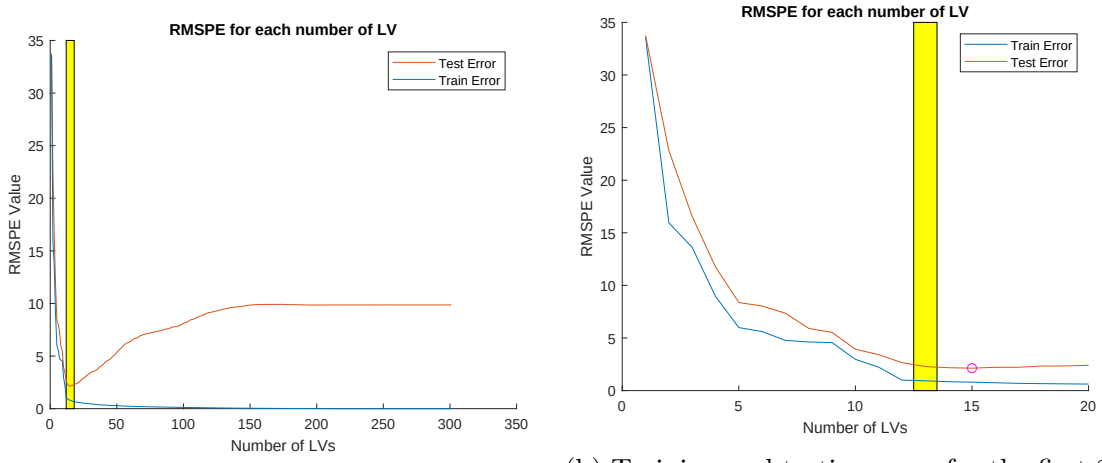

(a) Training and testing error for all LVs.

(b) Training and testing error for the first 20 LVs.

Figure 6.1: Training and testing error as a function of the number of LVs.

By using 13 LVs to predict all of the outputs, shown in Figure 6.2, the RMSPE values for the burnup, enrichment, and cooling time predictions are 0.57%, 1.69%, and 4.60%, respectively. The predicted values are all within 1 GWd/MTU, 0.25% U-235, and 2 years of the actual burnup, enrichment, and cooling time values, respectively.

These results are comparable to the results of the PCR models constructed based on cross validation. When the prediction errors are examined closely, the burnup predictions contain a bias to under predict values of 40 and 70 GWd/MTU. The enrichment predictions show a slight increase in the prediction variance as the value being predicted increases, but there is no consistent bias. Finally, the cooling time predictions show the intermediate values, 15 and 20 years, have the lowest prediction variance, but they each contain a bias. Values of 15 and 30 years are usually under predicted and values of 20 years are over predicted. The bias

on values of 20 and 30 years has been seen in previous models. The burnup and enrichment predictions both have RMSPE values below 5%, so they meet the accuracy requirement. Only 7.3% of the cooling time predictions are more than 1 year away from the actual value of the observation, which is the lowest percentage observed in any model thus far.

The condition number of this model 1, which is well within the threshold to be considered stable and the minimum possible value. This condition number is not surprising, however. In the calculation of the condition number, as described in Chapter 3, it is a ratio of the singular values of the matrix being inverted, $(t_i)^T * (t_i)$ in the case of PLS. The size of this matrix is 1×1, since only 1 LV is used in the inner transformation at a time. Therefore, the condition number is the ratio of the singular value of a 1×1 matrix to itself, which will always be 1. This calculation also shows that the matrix being inverted will always be a single value, which is known to be stable. Based on this, the condition number of all PLS models will always be 1 and will be stable.

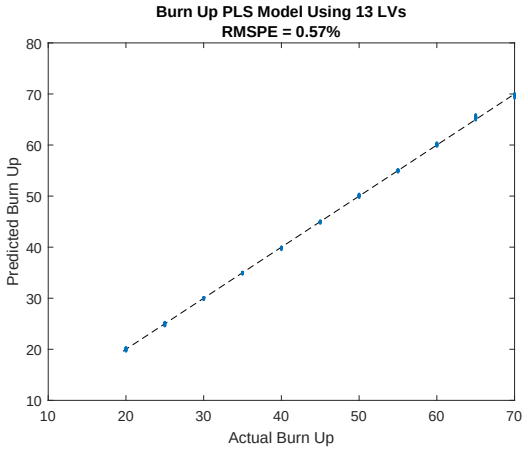

(a) Predicted vs actual values of burnup.

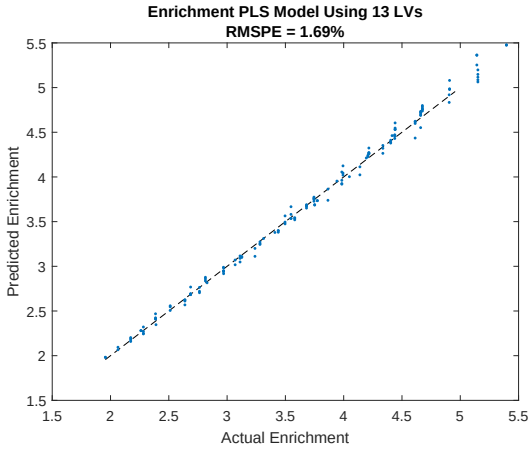

(b) Predicted vs actual values of enrichment.

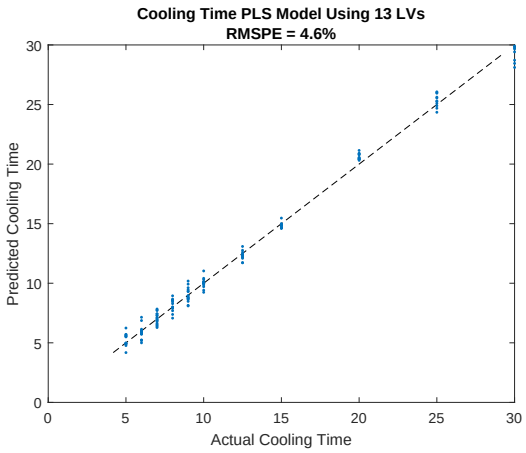

(c) Predicted vs actual values of cooling time.

Figure 6.2: Comparison of actual and predictions for multilinear PLS model.

6.2 Akaike Information Criteria PLS

The next set of models built is based using the number of LVs suggested by the use of AIC, similar to Section 5.5. The impact of the output data on the outer transformation of the input data results in calculating AIC values for each output separately, shown in Figure 6.3. These values show a similar trend as the values calculated for PCR; they continually

decrease as a function of the number of LVs. Therefore, this was also treated similar to a scree plot, and the middle of the bend was taken as the appropriate number of LVs to use. This is estimated to be at 25 LVs for all outputs.

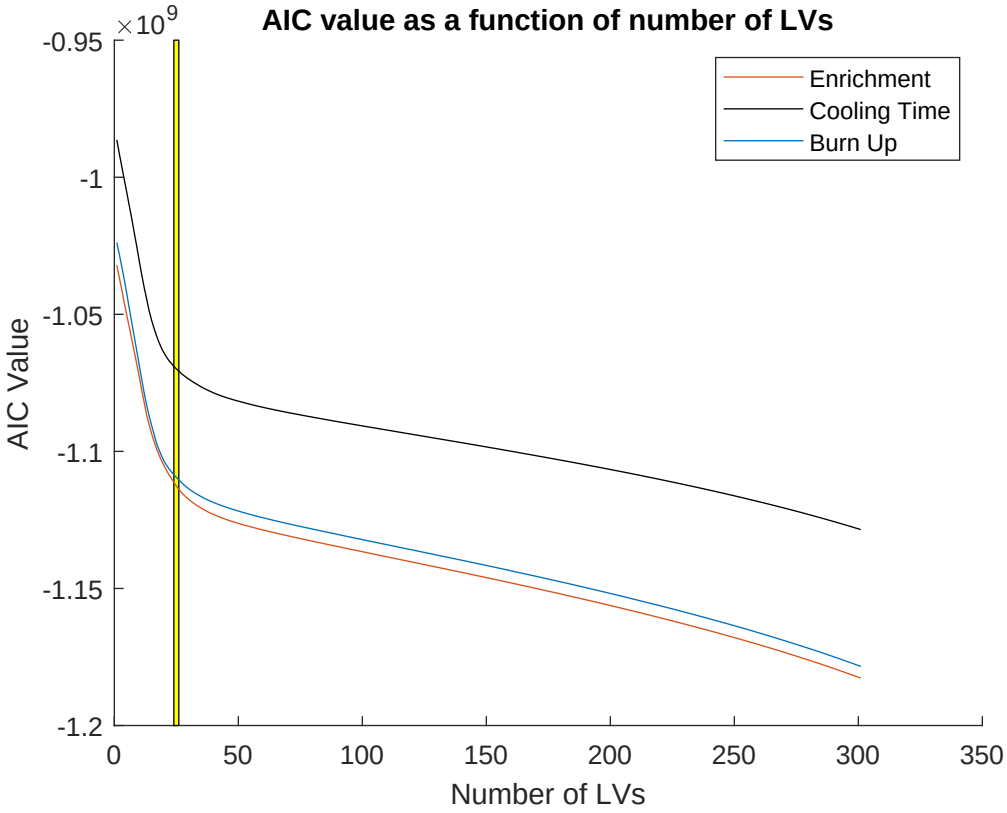

Figure 6.3: AIC values as a function of LVs used in PLS for each output.

When these models are used to predict the output data, they also show good prediction performance. The RMSPE for the burnup, enrichment, and cooling time predictions are 0.57%, 2.08%, and 8.11%, respectively. Predicted values are all within 1 GWd/MTU, 0.5% U-235, and 5 years of the actual burnup, enrichment, and cooling time values, respectively. The prediction errors are mostly similar to the other well predicting models that have been created, but the cooling time error is higher. The consistency of PLS models having low prediction error supports that correlations between variables are reduced and the assumptions of the OLS performed are better met. None of the predictions show consistent bias, even the cooling time values that have previously had biases. In the cooling time

predictions, it is observed that the prediction variance decreases as the value being predicted increases, until an actual value of 25 years, at which point the variance begins to increase. The burnup and enrichment predictions of this model also meet the accuracy requirement since their RMPSE values are below 5%. For the cooling time predictions, 17.9% of the predictions are more than 1 year away from the actual value. While this is lower than some of the PCR models, the previous PLS model had a lower percentage. Therefore, the previous PLS model would be favored for the prediction of the cooling time.

The condition number for each of these models is 1, which means that the models are stable.

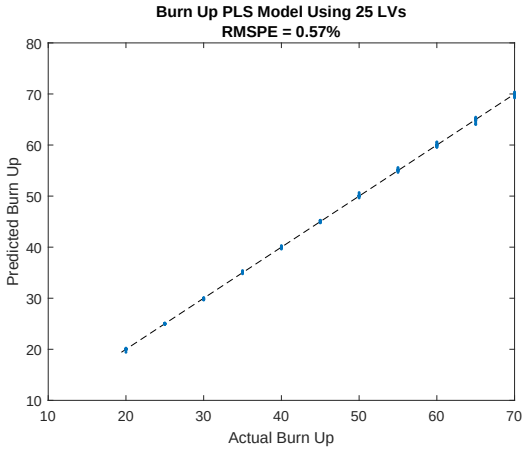

(a) Predicted vs actual values of burnup.

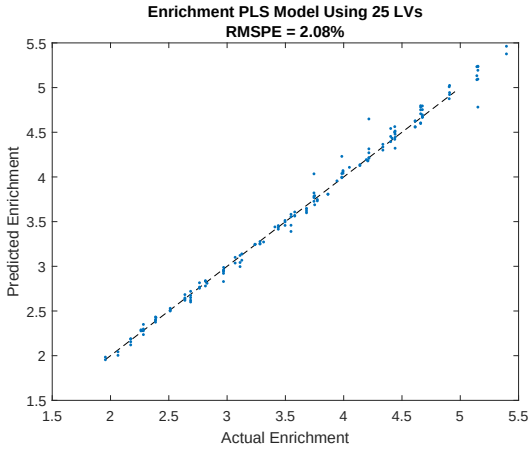

(b) Predicted vs actual values of enrichment.

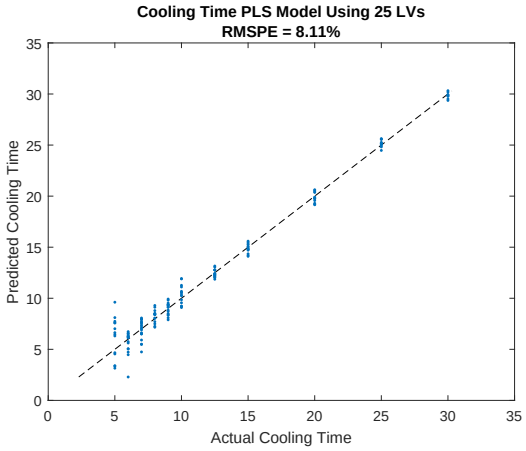

(c) Predicted vs actual values of cooling time.

Figure 6.4: Comparison of actual and predictions for PLS model based on AIC

.

6.3 Cross Validation

The next set of models built is based on the cross validation of the testing error with the addition of each LV, as shown in Figure 6.5. The highlighted section of Figure 6.5a shows that the minimum RMSPE values for each output occurs at less than 20 LVs. When this

section is closely examined, Figure 6.5b, the minimum RMSPE values are found to occur at 18, 15, and 13 LVs, as indicated by the magenta circles. However, similar to the PCR cross validation and multilinear PLS models, the errors begin to flatten at 13 LVs, shown by the highlighted section of Figure 6.5b. Due to the expected stability of both models based on the PLS algorithm, the 13 LV models were chosen for this method for their simplicity.

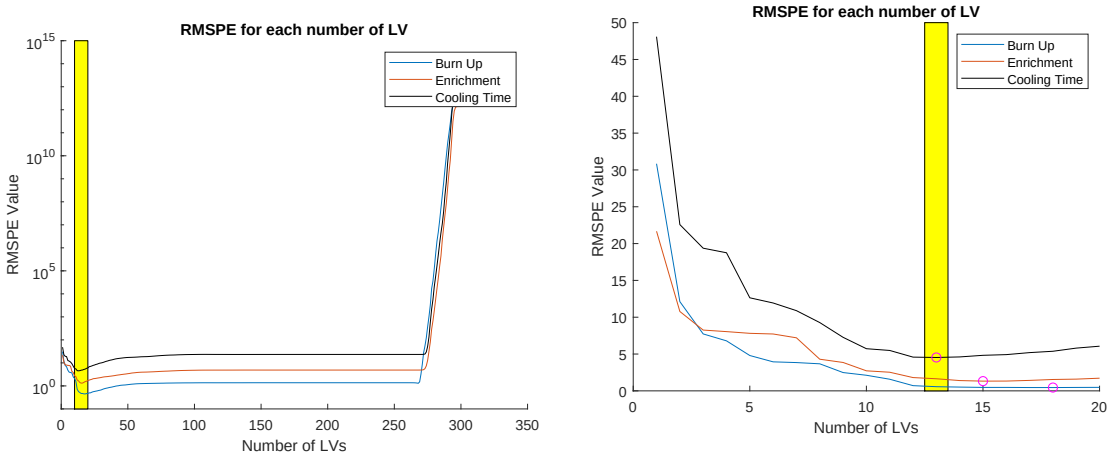

(a) Training and testing error for all LVs.

(b) Training and testing error for the first 20 LVs.

Figure 6.5: Training and testing error as a function of the number of LVs.

When these models were used to predict the testing data, Figure 6.6, the RMSPE values are 0.57%, 1.64%, and 4.53%, respectively. The predicted values are all within 1 GWd/MTU, 0.25% U-235, and 2 years of the actual burnup, enrichment, and cooling time values. The burnup predictions show a bias in under predicting values of 40 and 70 GWd/MTU, and over predicting values of 65 GWd/MTU. The enrichment predictions do not show any consistent biases. The cooling time predictions contain biases that are present in many of the other models. Values of 20 years are over predicted, and values of 30 years are under predicted. This model has a lower RMSPE and uses 7 fewer LVs than the PLS AIC model, but the PLS AIC model does not contain these biases. This suggests that the information contained in those additions 7 LVs removes the biases but adds additional noise to the predictions to increase the RMSPE. The burnup and enrichment predictions meet the accuracy requirement, with RMSPE values less than 5%. For the cooling time predictions, 7.3% of all predictions are more than 1 year away from the actual value, same as

the Multilinear PLS model. The condition number of each of these models is 1, as previously explained.

Each of these models use the same number of LVs that are used in the multilinear PLS model, but the enrichment and cooling time predictions have slightly lower RMSPE values. This difference exemplifies how the output used in PLS has an impact on the calculations of the calculated scores and the predictions of the model.

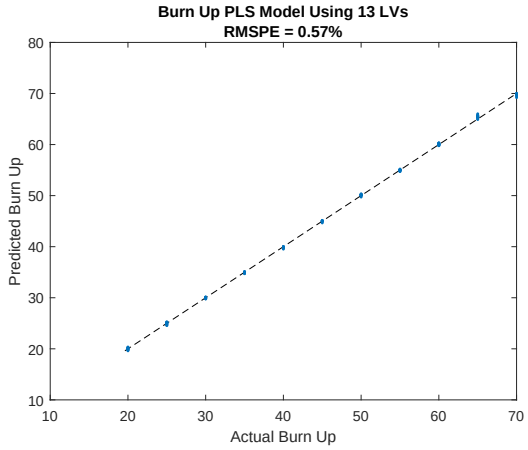

(a) Predicted vs actual values of burnup.

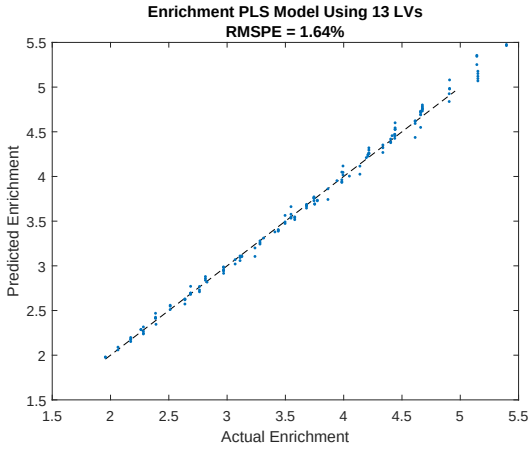

(b) Predicted vs actual values of enrichment.

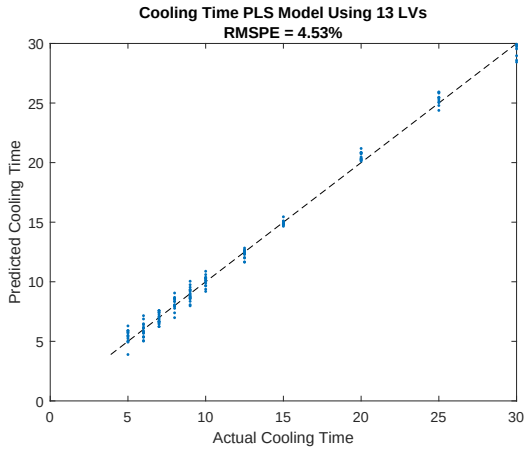

(c) Predicted vs actual values of cooling time.

Figure 6.6: Comparison of actual and predictions for PLS model based on cross validation.

6.4 Nonlinear PLS

The final model constructed in this work is a nonlinear PLS model to predict only the cooling time. By examining the input and output scores of the first LV for the burnup and enrichment prediction models, Figure 6.7, there is not a clear nonlinear relationship. Therefore, a nonlinear PLS model would not be expected to perform better than the linear ones, so were not considered.

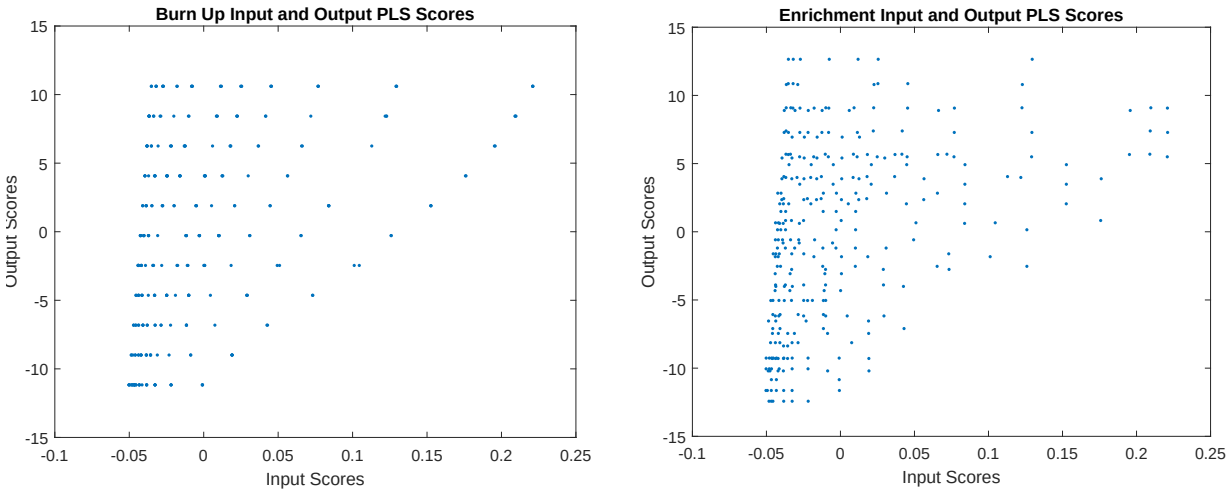

(a) Scores to predict the burnup

(b) Scores to predict the enrichment

Figure 6.7: Input and Output Scores of the first LV to predict burnup and enrichment.

However, as Figure 6.8 shows, there is a clear nonlinear relationship between the input and output scores for cooling time. This relationship contributes to the higher prediction errors for this variable and suggests that a nonlinear PLS model may decrease the prediction error because the regression would be able to capture more of the relationship between the input and output. A nonlinear PLS model can be built by fitting a nonlinear function or non-parametric model directly to the input and output scores. However, for optimal results this requires a unique function or model for every LV included in the cross validation. If it is unclear what nonlinear function would best capture the behavior, then this can introduce additional errors into the model. It was decided to train artificial neural networks to fit each function to remove this possible source of error and ensure that the best fit for each set of LV scores was found. Neural networks utilize layers of interconnected nodes to pass

information and relate inputs to a desired output, similar to a biological nervous system [45]. Each node sums weighted inputs, subtracts this value from a given threshold, then passes the result through a prescribed nonlinear function. Neural networks can be used for a variety of purposes, including classification, pattern recognition, and numerical predictions. The weights are initially randomized then optimized based on gradient descent for this work, meaning that this model does not involve matrix inversion and multiple sets of networks had to be trained and compared to ensure that a global minimum for the prediction error was found.

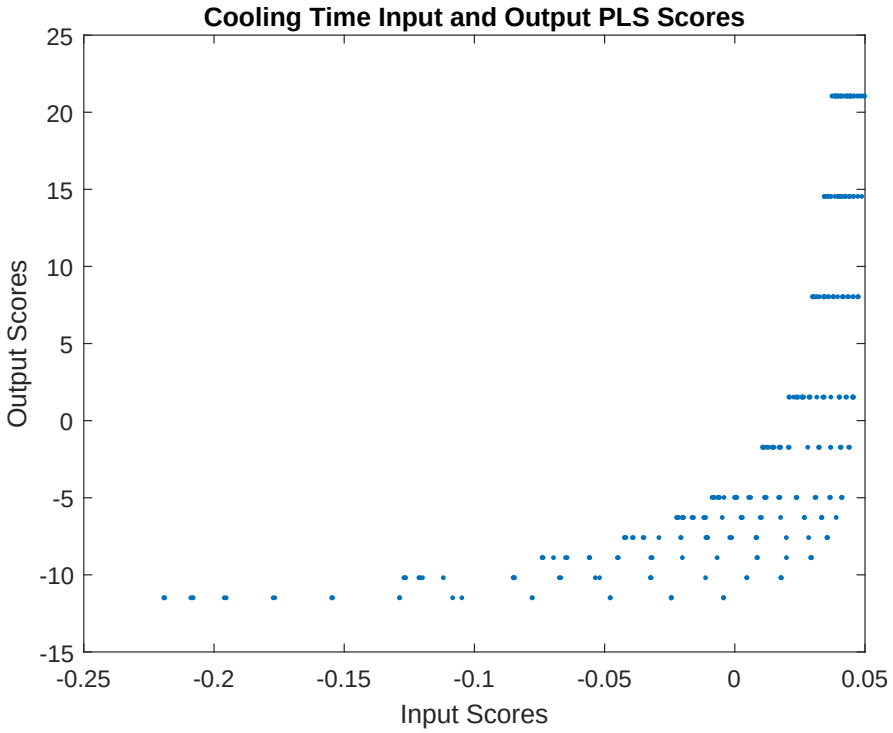

Figure 6.8: Input Scores vs Output Scores of the first LV to predict cooling time.

To build the nonlinear PLS model, the methodology outlined in Qin and McAvoy [41] was implemented. A linear outer transformation was constructed using the NIPALS algorithm [37] and a neural network was used to perform the inner transformation. A different network was built and trained for each LV, totaling to 20 networks being constructed, using the same architecture: a feedforward network with 1 hidden layer, 1 neuron per layer and a

hyperbolic tangent sigmoidal transfer function. Other activation functions were considered, such as log-sigmoidal, but the hyperbolic tangent sigmoidal function performed the best.

Cross validation was also used with this model to determine the number of LVs to use, shown in Figure 6.9. Based on the results of the previous PLS models and to conserve time in creating and training the neural networks, this model was restricted to 20 LVs. For this model, the minimum error using the testing data is at 11 LVs, shown by the highlighted section.

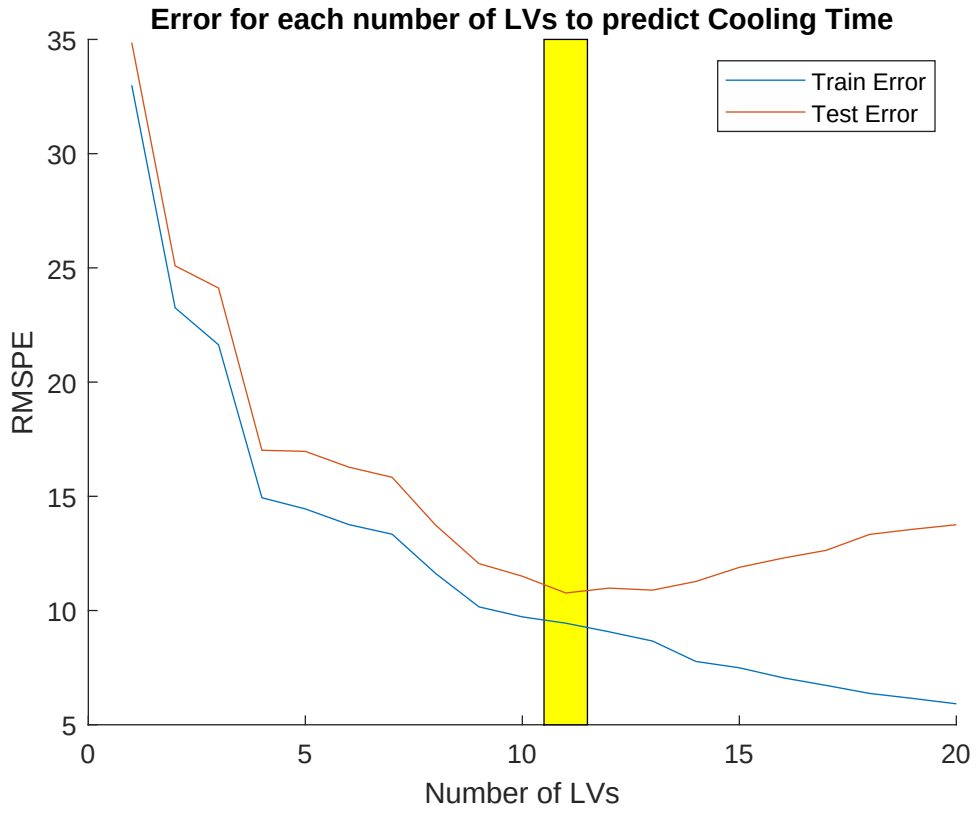

Figure 6.9: Cross validation for nonlinear PLS model to predict cooling time.

When this model was used to predict the cooling time of the fuel, shown in Figure 6.10, the RMSPE is 10.77%. All of the predictions are within 3 years of the actual value. Values of 20 years are always over predicted and values of 30 years under predicted, similar to what has been observed with other models. The RMSPE of this model is more than twice the

RMSPE of the linear PLS model. Over half, 52.98% of the predictions are more than 1 year away from the actual value. This means that this model has the highest percentage of predictions outside the accuracy requirement of any PLS model and is not an ideal model to use for safeguards. Since neural networks do not utilize matrix inversion, there is no condition number for this model.

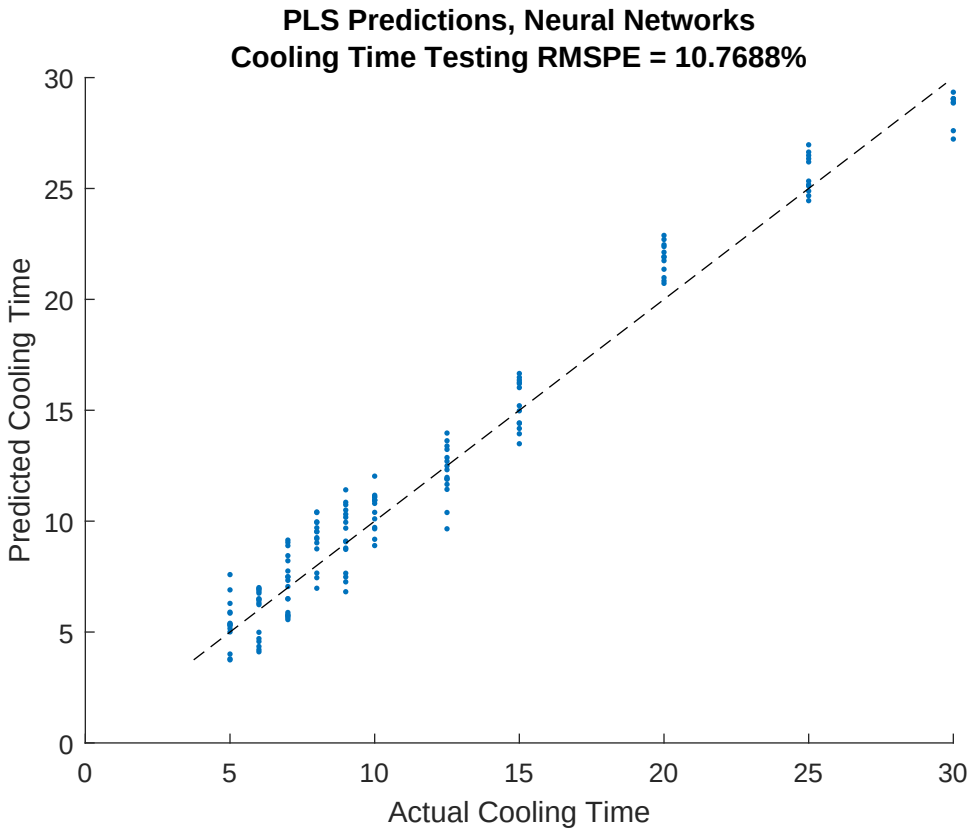

Figure 6.10: Predicted vs. Actual cooling time results using the nonlinear PLS model.

The prediction results of this model seem counter intuitive of the expectation that this model would have a lower RMSPE, but a comparison of the cross validation for the linear and nonlinear PLS models helps to highlight possible reasons for this result. As Figure 6.11 shows, using just the first LV in the nonlinear model has a significant decrease in the RMSPE compared to the linear model, 35.5% vs 49.3%. However, there is a large difference in the change in error when the second LV is used: the linear model has a decrease of 26% while the nonlinear model has a decrease of about 10%. This indicates that the information contained

in the second LV of the linear model contains more information about the output space than that of the nonlinear model. This is a trend that continues through the first few LVs in each of the models: there is a larger decrease in the RMSPE with the addition of each LV for the linear model than the nonlinear model. The trend appears to continue until the minimum RMSPE is reached for each model. The trend and results shown in Figure 6.11 leads to the conclusion that nonlinear transformation is able to capture more of the information about the data into the first LV. However, by placing more information into the first LV, the other LVs do not contain as much information as they do in the linear model. The later LVs in the nonlinear model begin to add in more noise to the predictions, increasing the error of the predictions. This explanation is supported by the larger difference between the testing and training error of the nonlinear model than that of the linear model. The difference between these errors is typically attributed to overfitting the model to the training data, since the first LV is able to explain a much larger portion of the data.

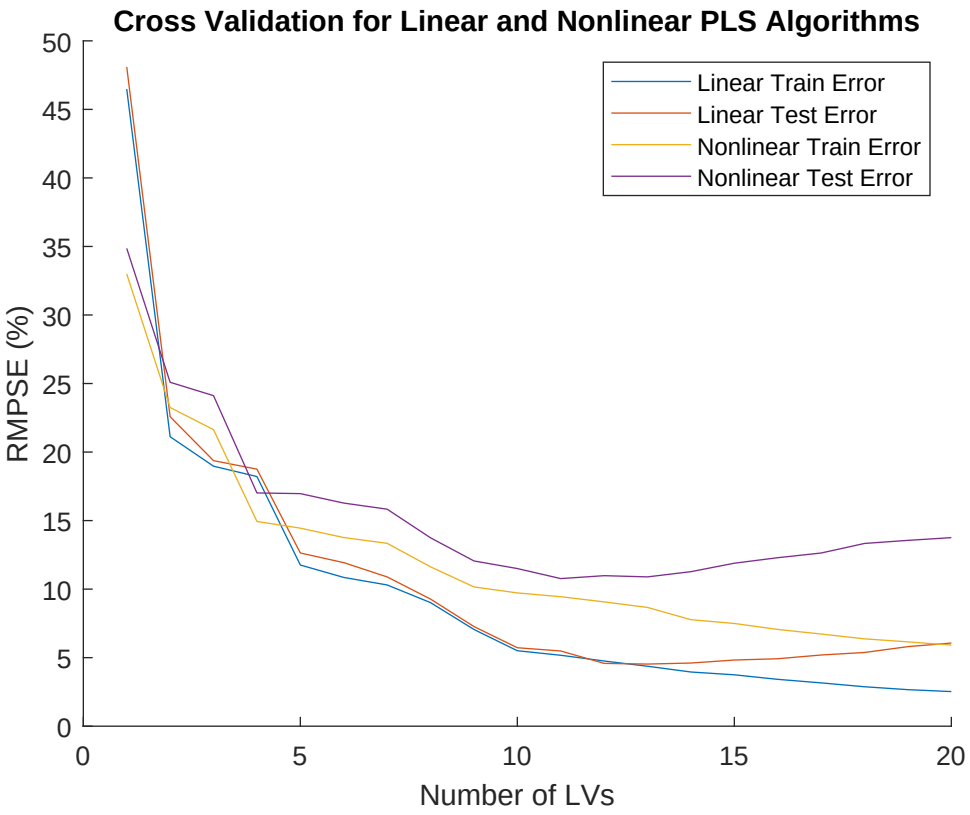

Figure 6.11: Cross validation of linear and nonlinear PLS models as a function of the number of LVs used.

Chapter 7

Model Selection and Uncertainty Quantification

7.1 Model Selection and Validation

The characteristics of each model to predict the burnup, enrichment, and cooling time are in Tables 7.1, 7.2, and 7.3, respectively. From these tables, there are four main trends observed from the performance of each technique. First, OLS has the highest condition number and the least stability. This matches expectations, since the PCR and PLS models are able to remove some of the correlation of the input data to better meet assumption 4 of OLS. Second, the PCR models show a trade-off between stability and prediction performance. This highlights a limitation of PCR when used with data that is correlated in a similar manner. Much of the information about the input data is placed in the first few PCs, but the later PCs are needed to provide an accurate prediction of the output space. This leads to the use of PCs with large and small eigenvalues, causing instabilities in the model. Third, the cooling time predictions always have the highest RMSPE values. This can be attributed to its known underlying nonlinear relationship between this characteristics and radiation signatures. Finally, the RMSPE of the burnup predictions are usually the lowest of the three characteristics. This is not unexpected, as this characteristic has been shown to have a linear relationship with the concentration of fission products [5], which means it has a linear relationship with certain energy bins of a gamma spectrum. Also, the burnup values used are at discrete values and are paired with multiple combinations of enrichment and cooling time values that allow the regression parameters to encapsulate many variations in the radiation

signatures that correspond to the same burnup value. The enrichment predictions usually have a higher RMSPE value, despite the actual values being calculated based on the burnup values because of the additional variation in the enrichment values.

Throughout each of these models there are some consistent biases in the cooling time predictions between the models. The multilinear, cross validation, and nonlinear PLS models, the AIC, cross validation, and eigenvalue based PCR models, and the OLS model all over predict cooling time of 20 years. All of the PCR models, the OLS and the cross validation and nonlinear PLS models under predict cooling times of 30 years. It is not surprising that the larger cooling time predictions exhibit more bias than the smaller values, as there are fewer isotopes present in the fuel, which results in fewer distinct emission signals in the gamma spectrum. It is likely that the fewer differences in the input space is leading the models to predict towards median value in this range, which is why predictions of 25 years do not exhibit a bias.

Table 7.1: Summary of results of each model to predict burnup

Model	No. Variables	RMSPE	Condition Number
OLS	12	3.51	9.35×10^{37}
PCR, Variance Explained	1	31.27	1
PCR, Eigenvalues	4	7.45	150.8
PCR, Correlation	1	26.59	1
PCR, AIC	14	0.61	1.72×10^{8}
PCR, Cross Validation	17	0.59	7.03×10^{8}
PLS, Multilinear	13	0.57	1
PLS, AIC	25	0.57	1
PLS, Cross Validation	13	0.57	1

The best model from this work is determined by a balance between the RMSPE of the predictions, ability to meet the accuracy requirements, and the condition number of the model. The burnup and enrichment predictions must be within 5% and the cooling times must be within 1 year of the actual value. A strict upper threshold of 100 is applied to the condition number. The stability criterion disqualifies the OLS, PCR based on eigenvalues, PCR based on correlation for cooling time, PCR based on AIC, and PCR based on cross validation. Each of these models has a condition number higher than the threshold.

Table 7.2: Summary of results of each model to predict enrichment

Model	No. Variables	RMSPE	Condition Number
OLS	12	4.32	9.35×10^{37}
PCR, Variance Explained	1	21.96	1
PCR, Eigenvalues	4	8.23	150.8
PCR, Correlation	1	19.16	1
PCR, AIC	14	1.78	1.72×10^{8}
PCR, Cross Validation	19	1.72	8.83×10^{8}
PLS, Multilinear	13	1.69	1
PLS, AIC	25	2.08	1
PLS, Cross Validation	13	1.64	1

With regards to the accuracy of the predictions, most of the models for burnup and enrichment predictions meets the 5% RMSPE threshold except for the PCR models based on percent variance explained, eigenvalues, and correlation. For the cooling time predictions, no model yields predictions that are all within 1 year of the actual value. However, some models are able to yield less than 10% of predictions greater than 1 year, with the PCR models based on AIC and cross validation yielding the lowest at 6.62%. Despite having the lowest percent of predictions outside 1 year of the actual value, this model does not have the lowest RMSPE value and contains biases in the predictions.

When the stability and accuracy criteria are combined, only the PLS models yield accurate prediction results and are stable. This highlights the ability of PLS to provide accurate and stable predictions for highly correlated data. Between the PLS models, the cross validation models have the lowest RMSPE values for the burnup and enrichment predictions and the multilinear model has the lowest RMSPE value for the cooling time. They have the same percent of cooling time predictions within 1 year of the actual value. The PLS cross validation models are selected as the best model over the multilinear PLS for each of the characteristics. This is because it yields the lowest RMSPE for the burnup and enrichment predictions and the lower condition number. This model does produce a slightly higher RMSPE value for the cooling time predictions, but they produce the same percentage of predictions within 1 year of the actual value which indicates that the difference in RMSPE is not significant.

Table 7.3: Summary of results of each model to predict cooling time

Model	No. Variables	RMSPE	$> \pm 1$ yr	Condition Number
OLS	12	8.55	41.7%	9.35×10^{37}
PCR, Variance Explained	1	48.36	90.7%	1
PCR, Eigenvalues	4	20.48	70.9%	150.8
PCR, Correlation	1	48.36	90.7%	1
PCR, AIC	14	4.72	6.62%	1.72×10^{8}
PCR, Cross Validation	14	4.72	6.62%	1.72×10^{8}
PLS, Multilinear	13	4.60	7.3%	1
PLS, AIC	25	8.11	17.9%	1
PLS, Cross Validation	13	4.53	7.3%	1
PLS, Nonlinear	11	10.77	53.0%	N/A

When the PLS cross validation model is used to predict the validation data set, the predictions have RMSPE values of 0.60%, 1.62%, and 4.61% for the burnup, enrichment, and cooling time, respectively as shown in Figures 7.1, 7.2, and 7.3. The predicted values are all within 1.2 GWd/MTU, 0.2% U-235, and 2.5 years of the actual value of burnup, enrichment, and cooling time, respectively. These values are similar to what was observed with the testing data set, which is due to the stability of the model preventing small changes in the input data from causing large changes in the output data.

The burnup predictions, Figure 7.1, have a bias to over predict values of 20 and 65 GWd/MTU and under predict values of 70 GWd/MTU. The first two biases were not observed with the testing data set. The enrichment predictions, Figure 7.2, have more noise than the burnup predictions, but do not contain any consistent biases. The residuals appear to be well centered around 0, as Figure 7.2b shows. Both the burnup and enrichment predictions have RMSPE values less than the 5% threshold. Finally, the cooling time predictions, Figure 7.3, are similar to the results of this model with the testing data. The lower values have random noise in the predictions, values of 20 years are over predicted, and values of 30 years are under predicted. 12.50% of the predictions are more than 1 year away from the actual value, which is almost twice the percent when this model was used with the testing data.

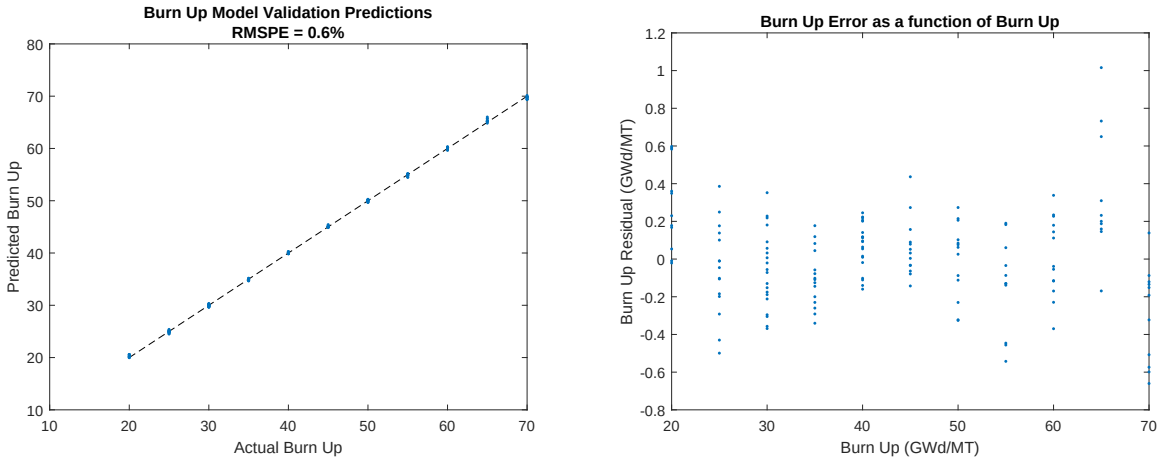

(a) Predicted values as a function of actual value. (b) Prediction error as a function of actual value.

Figure 7.1: Validation data predictions of burnup.

The prediction results of these models is similar to what has been observed in previous work. Errors in burnup predictions from previous empirical modeling efforts are 0.07% [6], 0.09-0.42% [7], 0.4-3.5% [22], 0.29-2.18% [31] and 3.9% [32]. Some of these errors are less than the RMSPE of the burnup predictions in this work but are similar and show that this model produces consistent results with other PLS models. It is noted that the errors that are lower come from PLS models, while the higher modeling errors are from PCR models. This strengthens the conclusion that PLS models perform better for fuel characterization. A more realistic input space, such as measured emissions, would be needed to provide an accurate comparison with current NDA methods.

For the enrichment predictions, previous empirical models have resulted in errors of 1.69-10.94% [7] and 17.5% [23], from the actual value. This model results in an RMSPE that is lower than any of the previous work. This may be because the enrichment is correlated to the burnup of the fuel in this work, which has not been done in previous models. This correlation means that any relationships between the burnup and specific energy bins or the neutron counts that exist are now tied to the enrichment. Therefore, it is not surprising that this model yields a lower average prediction error than previous models.

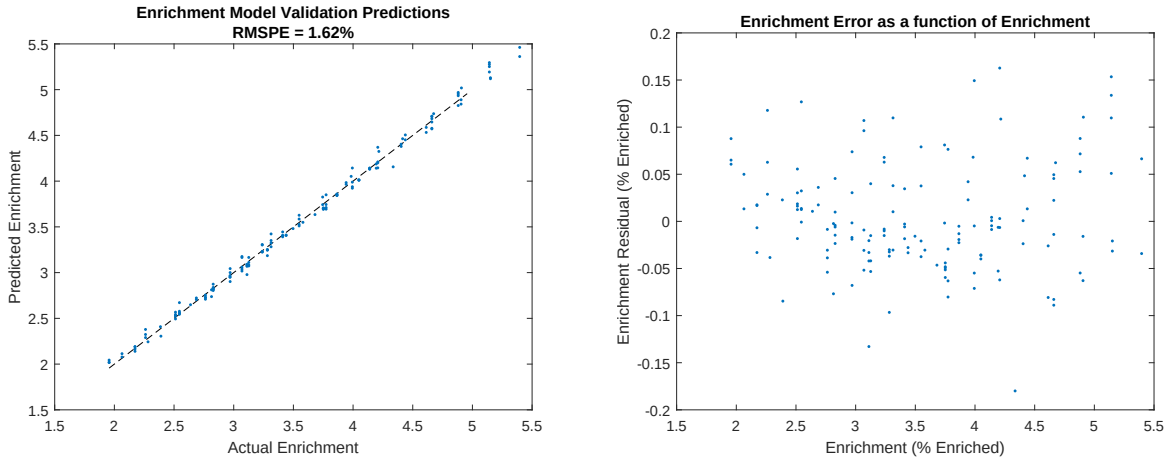

(a) Predicted values as a function of actual value. (b) Prediction error as a function of actual value.

Figure 7.2: Validation data predictions of enrichment.

Finally, previous empirical models have been able to predict cooling time values with 1.26-8.65% [7] and 1.8-13.3% [23] from the actual value. An RMSPE of 4.813% from the cooling time model is consistent with the errors of previous models and performs better than some.

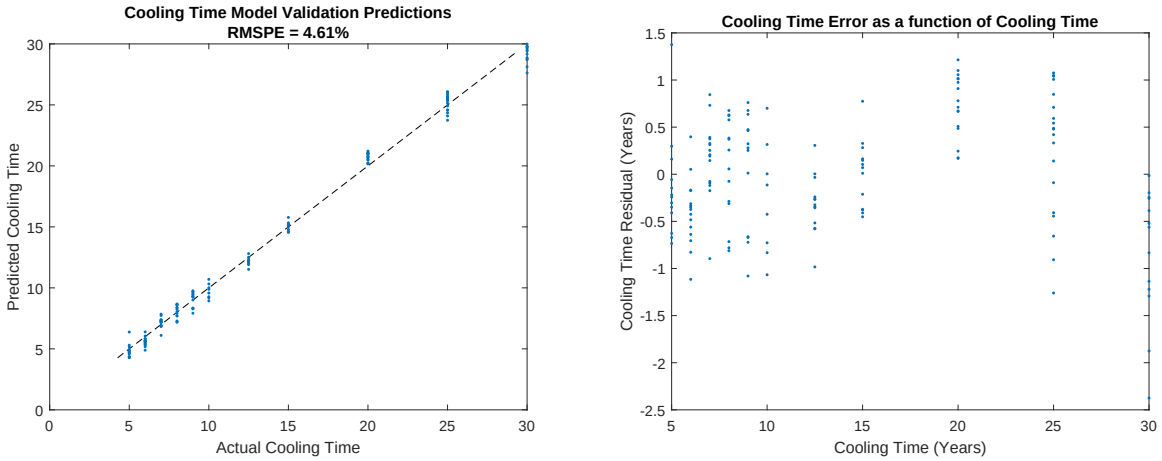

(a) Predicted values as a function of actual value. (b) Prediction error as a function of actual value.

Figure 7.3: Validation data predictions of cooling time.

7.2 Model Uncertainty Quantification

The prediction variance, bias, and total uncertainty of the cross validation PLS models were calculated to provide a prediction interval and understand if a predicted and actual value are statistically different. Figure 7.4 shows histograms of the relative prediction variances of the burnup and enrichment, Figure 7.4a, and the cooling time, Figure 7.4b. The cooling time variances are in a separate histogram due to the differences in scale between these variances and those of the burnup and enrichment predictions.

The burnup and enrichment relative variances are mostly less than 0.0001, which corresponds to prediction standard deviations less than 0.316 GWd/MTU and 0.0412% U-235. The enrichment relative biases are more spread out than those of the burnup, which is consistent with the enrichment predictions having a higher RMSPE value and more noise than the burnup predictions. The cooling time relative variances are two orders of magnitude larger than those of the burnup and enrichment, reaching as high as 0.0535 or an actual prediction standard deviation of 1.157 years. Most of the relative variances are within 0.0054, or 0.542 years.

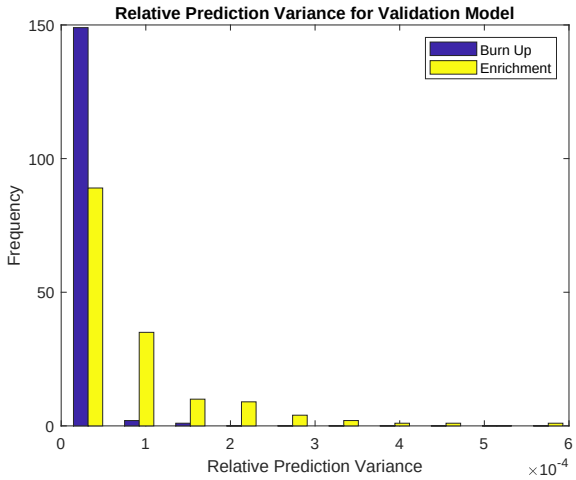

(a) Histogram of relative prediction variances for burnup and enrichment predictions.

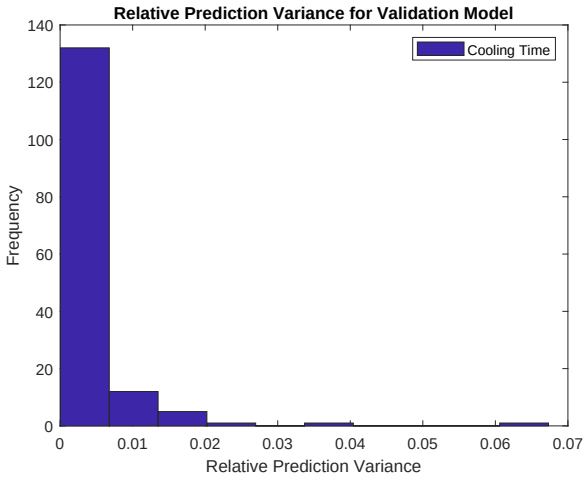

(b) Histogram of relative prediction variances for cooling time predictions.

Figure 7.4: Histograms of relative prediction variance using 500 samples of 100 observations of the validation data predictions.

The 95^{th} percentile of the calculated prediction variances was taken as the prediction variance for each of the output variables. This percentile yields a conservative estimate of the variance of the predictions, capturing 2 standard deviations around the mean. The resulting prediction standard deviations for the burnup, enrichment, and cooling time are 0.219 GWd/MTU, 0.0510% U-235, and 0.692 years, respectively.

Next, the bias of the predictions was calculated, with the relative biases shown in Figure 7.5. The cooling time values, Figure 7.5b, were again separated from those of the burnup and enrichment values, Figure 7.5a, to highlight the difference of scale. The burnup relative biases are within ±0.01, which corresponds to a bias of within ± 0.45 GWd/MTU, which is consistent with the errors seen in Figure 7.1b. The enrichment relative biases are more spread out than that of the burnup predictions, which is to be expected based on the larger range of the enrichment predictions shown in Figure 7.2a. The enrichment relative biases are all between -0.026 and 0.0304, corresponding to biases between -.114 and 0.111 % U-235 of the actual value. This range matches the range observed in Figure 7.2b well. Finally, the cooling time relative biases are an order of magnitude larger than those of the other characteristics. The values mostly range between -0.147 and 0.2, corresponding to biases of

-1.225 and 2.14 years. These values and the shape of Figure 7.5b suggest that the model for cooling time is more likely to over predict the actual values.

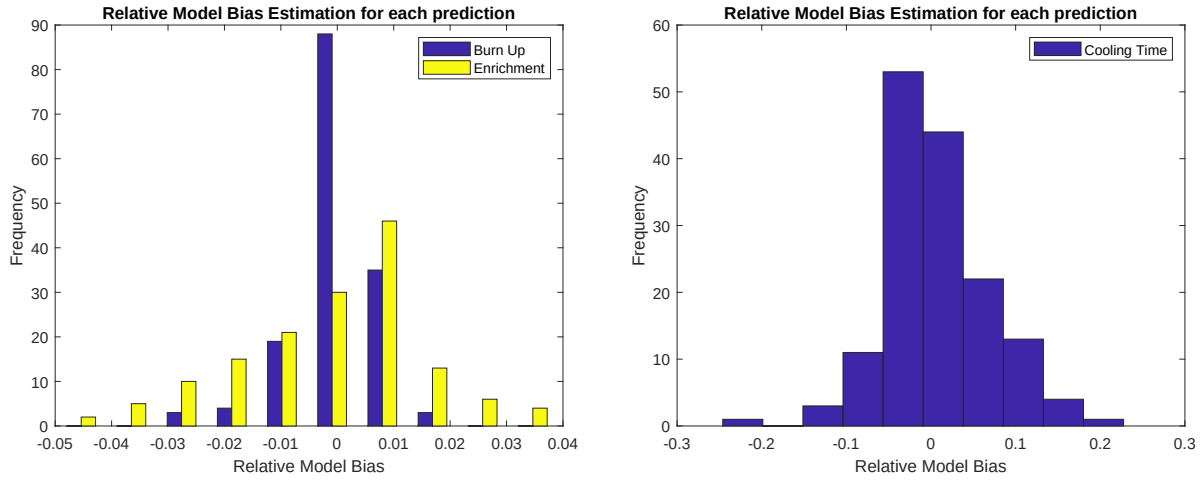

(a) Histogram of relative biases for burnup and enrichment predictions.

(b) Histogram of relative biases for cooling time predictions.

Figure 7.5: Histograms of relative biases for each predicted observation.

The means of the calculated biases are taken as the bias of each model. The resulting biases are 0.0009 GWd/MTU, -0.0033% U-235, and 0.048 years, for the burnup, enrichment, and cooling time, respectively. These values suggest that the burnup and cooling time models both have a tendency to over predict values, and the enrichment model has a tendency to under predict values although these are very small biases and contribute little to the total error.

The prediction variances and biases were combined using Eq. 3.6 to calculate the total uncertainty of each model. The uncertainties of the burnup, enrichment, and cooling time models are 0.220 GWd/MTU, 0.051% U-235, and 0.694 years (253 days), respectively. These correspond to between 0.31-1.10% uncertainty in the burnup predictions, 0.95-2.61% uncertainty in the enrichment predictions, and 2.3-13.87% uncertainty in the cooling time predictions.

When compared with the uncertainty of current methods, the burnup uncertainty is fairly low, and the cooling time uncertainty is high. In previous empirical modeling, Hellesen

et al. observed total errors of 4-5 MWd/kgU for burnup predictions, 0.6-2.4% U-235 for enrichment predictions, and 0.3-1 year for cooling time predictions when using experimental data [23]. Charlton et al. observed uncertainties of 7.6% for burnup predictions [32]. The models in this work have lower uncertainty than the uncertainty of most of the predictions by either of these previous works, which means that these models would more readily be able to discriminate between differences in declarations and predicted values. When compared to the average uncertainty in estimating cooling time using the Cs-134/Eu-154 isotopic ratio, less than 120 days [16], this model has a larger uncertainty, more than double.

The uncertainties of each model are then used to develop a prediction interval (PI) which is used to inform if a future prediction is within expectations. They can also be used to compare a predicted value to an operator declaration to determine if they are statistically different. A 95% PI is developed for these models, which corresponds to $\pm$ 1.6449 times the calculated uncertainty of each model. The PI is then used to indicate a false alarm, or when there is a stated significant difference between predicted and declared values stemming from model inaccuracy as opposed to inaccuracies in the declarations.

Figures 7.6, 7.7, and 7.8 show the results of how well the residuals of each predicted characteristic match the associated accuracy requirement. The markers show the residual of that observation, the error bars show the PI, and the dotted red lines show the accuracy requirement of the characteristic. By comparing the residual with the accuracy requirement and the residual $\pm$ the PI show the potential for a false alarm. The residual values show how well the predictions match the declarations, and the PI shows how often there is 95% confidence that the predicted value is within the accuracy criterion.

The percent residuals of the burnup predictions, Figure 7.6, are all within the 5% error criterion and all of the error bars are within the criterion as well. This indicates that there is 95% confidence that all of the predicted values are within 5% of the actual value, leading to a 0% false alarm rate for the burnup. The percent residuals of the enrichment predictions, Figure 7.7, shows that there is one observation outside the 5% error criterion, leading to a false alarm rate of 0.66%. However, there are 22 observations that do not have 95% confidence that they are within 5% of the actual value, leading to a false alarm rate of 14.47%. Finally, the absolute residuals of the cooling time predictions, Figure 7.8, shows that there are 19 observations that have residuals more than 1 year from the actual value, leading to a false alarm rate of 12.5%. Most of these observations have actual values of 20-30 years, indicating that the higher cooling time values are predicted least accurately. The relatively large uncertainty of the cooling time predictions leads to a PI of 1.14 years

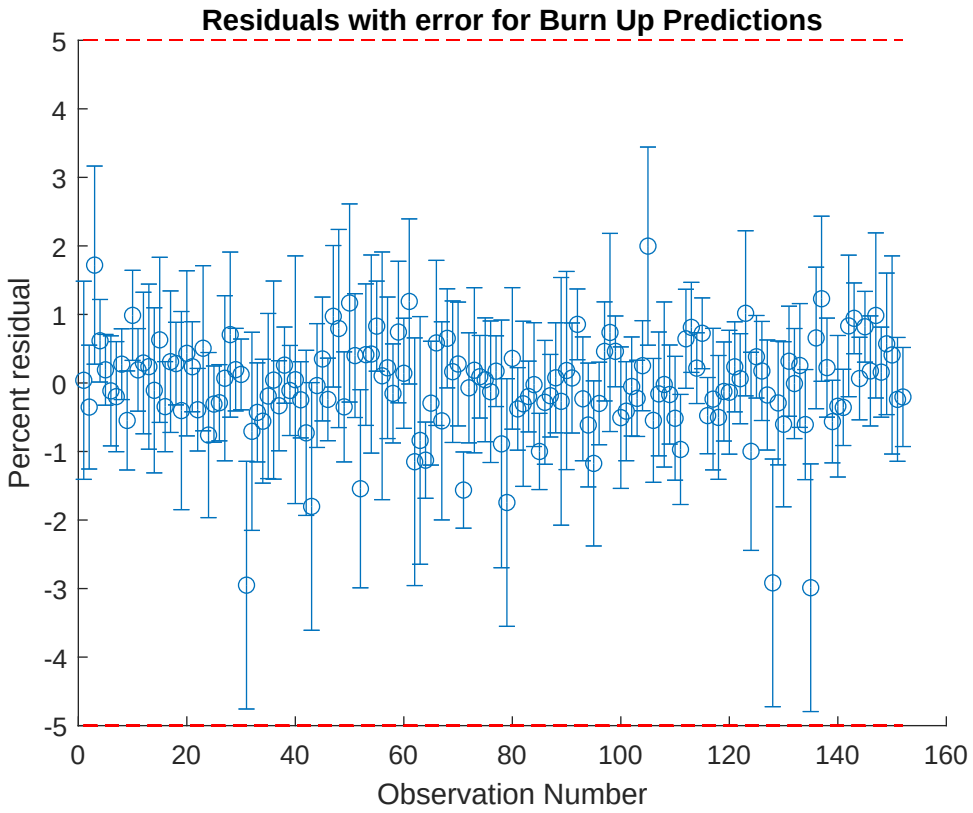

Figure 7.6: 95% Prediction Interval applied to residuals of burnup predictions. The red line is the PI and the error bars are the calculated uncertainty for the burnup predictions.

means that none of the observations have 95% confidence that they are within 1 year of the actual value. This results in a false alarm rate 100%.

The false alarm rates of the residuals and the 95% confidence of the predictions show that these models are able to achieve consistently accurate results of the burnup with 95% confidence. However, there are false alarms with regards to the enrichment and cooling time predictions, which limits this methodology's application for safeguards inspections.

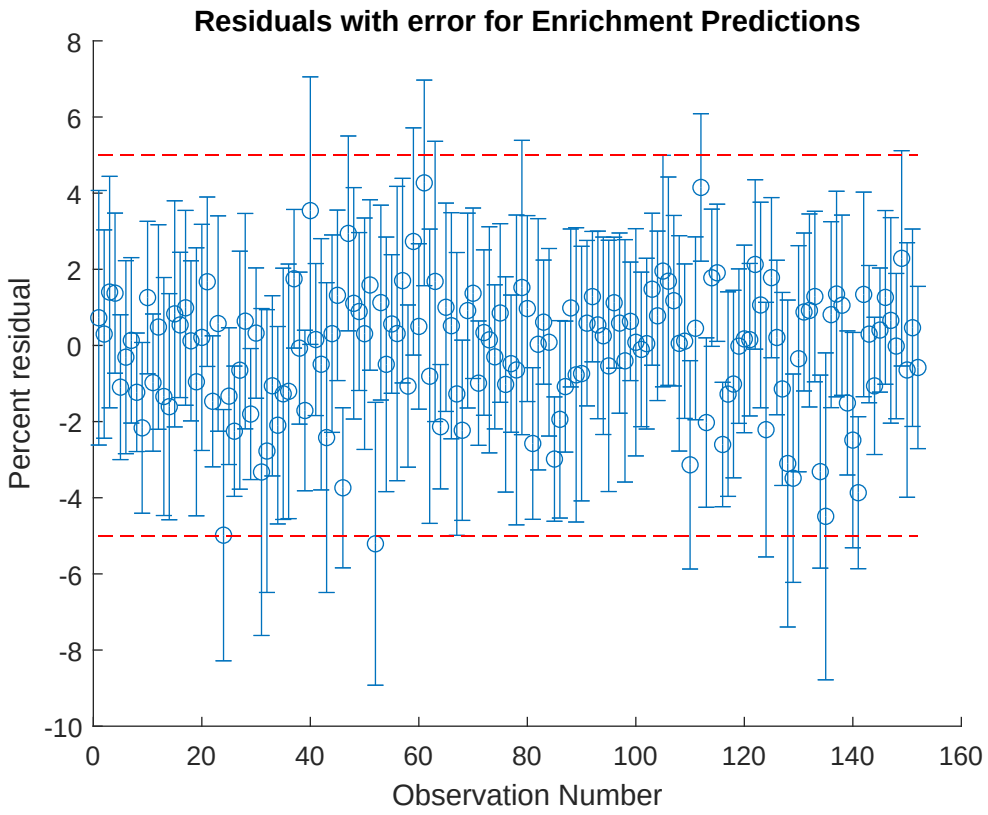

Figure 7.7: 95% Prediction Interval applied to residuals of enrichment predictions. The red line is the PI and the error bars are the calculated uncertainty for the enrichment predictions.

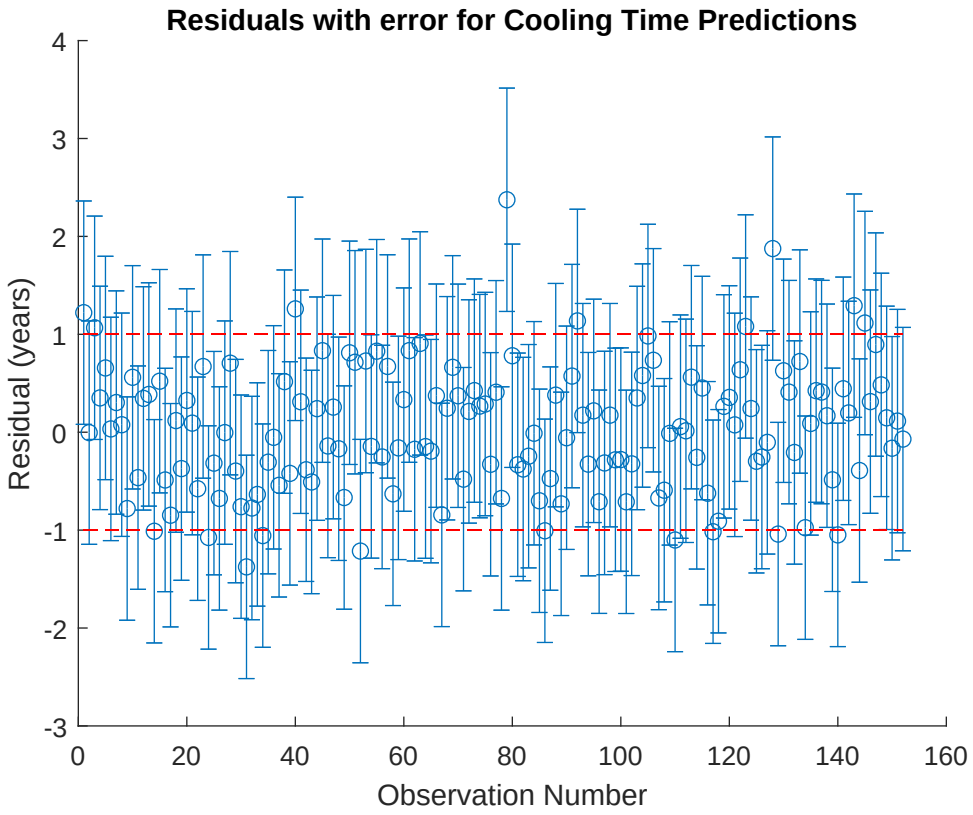

Figure 7.8: 95% Prediction Interval applied to residuals of cooling time predictions. The red line is the PI and the error bars are the calculated uncertainty for the cooling time predictions.

Chapter 8

Conclusions

The ability to accurately characterize used nuclear fuel has a large impact on the ability to independently verify fissile material quantities and operator declarations for nuclear safeguards. Current methods to perform this characterization are often limited by the ability to measure emissions from a select few isotopes contained in the fuel. To overcome the challenges associated with this, various efforts have been made to explore the ability of empirical modeling to estimate the burnup, initial enrichment, and cooling time of UNF based on a larger number of isotopes or the entire gamma spectrum emitted by the fuel. This work expands upon these prior efforts by using the gross neutron counts in addition to the gamma spectrum to predict each of the desired characteristics. This work also provides a comparison of different modeling techniques and methods to determine the number of variables for dimensionality reduction techniques.

The methods used to perform this modeling are all linear based parametric models, Ordinary Least Squares Regression (OLS), Principal Component Regression (PCR), and Partial Least Squares Regression (PLS), evaluated based on their prediction accuracy and stability. Methods to determine the number of variables to use in PCR and PLS include the amount of variance explained, eigenvalues, correlation to the output to be predicted, Akaike Information Criteria, and cross validation. The PLS models consistently had the best prediction performance and stability. This is attributed to the transformations used in this technique collapsing correlations in the input and output data into the same latent variable to reduce the correlation between latent variables. The stability of PLS, when used to predict a single output, is attributed to the inversion of a single number during the inner transformation. The PCR models exhibited a trade-off between accurate predictions and

stability. This is attributed to the input data being correlated in very similar directions, placing most of the information into the same PC, despite the later PCs containing most of the information about the output data.

The best model was determined to be PLS models based on cross validation to predict a single output. These models generally have the lowest root mean square percent error (RMSPE), a condition number of 1, and met the accuracy requirements the best of the models. When used to predict the validation data set, these models result in RMSPE values of 0.60%, 1.62%, and 4.61% for the burnup, enrichment, and cooling time predictions, respectively. The cooling time predictions always have the largest error of the three characteristics, with the later cooling times having the largest error due to the decrease in changes in the signatures. This may not be of great concern when applied to safeguards. Currently, the ability to quantify the cooling time of an assembly is used to improve the estimate of the burnup. If the burnup is able to be estimated using a method independent of the cooling time, it becomes less important to accurately predict the cooling time for verification of the fissile material. These prediction errors are similar to what has been seen with previous empirical modeling efforts, with the enrichment predictions performing better than previous models. The uncertainty of these models was calculated based on their prediction variances and biases. The total uncertainties are 0.220 GWd/MTU, 0.051% U-235, and 0.694 years for the burnup, enrichment, and cooling time models, respectively. The uncertainty of each model was found to be similar to those of previous modeling efforts and methods to characterize UNF. When the residual of each observation and its uncertainty are used with a prediction interval, the predictions of burnup, enrichment, and cooling time have a false alarm rate of 5.26%, 2.63%, and 1.38%, respectively. These rates show that even though some of the predictions seem to be similar to the actual value, they can still be significantly far enough away to raise an alarm.

The models created in this work show the strengths of empirical modeling in characterizing UNF for safeguards verification. However, they do have limitations. The primary limitation of this work is the use of radiation emissions from the fuel, as opposed to radiation detected from the fuel. The detected radiation can be measured in a physical system during a safeguards inspection. The radiation emissions cannot be directly measured. Radiation emissions have a higher intensity, more photopeaks, no shielding concerns, and no detector or measurement noise compared to the emissions that can be measured in a detector. These features contribute significantly to the accuracy of the predictions due to an increase in the amount of information available in the spectrum. It is unclear if the use of a detector signal would have a substantial effect on the multicollinearity of the input data, as it would

most likely contain fewer photopeaks, so there would be less correlation between photopeaks. However, other features of the spectrum would still be correlated to the photopeaks present, such as the Compton continuum or the Compton edge. Using a measured count would have increased uncertainty in the input space, due to counting statistics and background subtraction, than what is present in this work. This would lead to reduced accuracy and larger uncertainty in the predictions. Changing the model inputs to the measured gamma spectrum and neutron counts in a detector would decrease the accuracy of the predictions but provide more realistic models and predictions that could be used during a safeguards inspection.

An additional limitation includes the use of only one fuel assembly and reactor type. This is not a large limitation when applying this methodology to UNF at a reactor, since each reactor is likely to consistently use the same fuel assembly types. It is also likely that when applying the methodology, facility-specific models would be constructed to account for facility-specific background radiation and signatures in the training data. This lessens the need to include multiple reactor types in the training data since each model would only have to account for likely variations in UNF characteristics at a single facility. However, the lack of reactor type variation is a limitation for use at a reprocessing or storage facility, which would be expected to handle fuel from a variety of assembly and reactor types. Therefore, to provide accurate predictions, the training data would have to include likely variations in the fuel characteristics

Similarly, the lack of variations in the cycle history, while capturing normal operations, does not capture all likely operations of the reactor. Some isotope concentrations, such as Cs-134, are very sensitive to the cycle history of the assembly. By not accounting for variations in the cycle history when generating the input space, the models cannot account for how these variations in the emissions and how these are related to each of the characteristics. Therefore, the results of this work are only applicable to the specific operation used.

Finally, the uncertainties calculated for each of the models is a uniform value for all values to be predicted. The results of the validation data predictions show that there is not a consistent bias or variance in the predictions, and that some values are better predicted than others. Therefore, a uniform uncertainty does not accurately capture the uncertainty of every prediction the way a variable uncertainty would.

8.1 Future Work

There are many improvements that can be made to further this work and build off of it. With regards to the exact work done, this can include incorporating the errors associated with the gamma and neutron emissions from SCALE, which would be used as the noise variance of the model to provide a more realistic estimate of the total uncertainty. It would also be of use to quantify the uncertainty of each observation since there is a clear difference in the bias and prediction variance of each actual value. Additional modeling techniques could be used to explore their performance in predicting this system and reduce the prediction error of the cooling time. Techniques include Kernel Regression, locally weighted PLS models, such as used by Coble et al. [7], and Ridge Regression. This work can also be recreated using actual gamma and neutron counts from a detector system. These inputs would reflect what is actually observed during an inspection, include physical detector effects, include the noise variance in the measurements to reflect a more accurate uncertainty of the model, and provide a more realistic view of how these models would perform with data from an assembly.

Possible extensions of the work completed include the inclusion of the reactor type as a variable to be predicted and variations in the cycle history of the assembly. Including the reactor type as a characteristic to be predicted would expand the number of variables in the output data set and accounting for both of these parameters would increase the observations of the input and output data. Including the reactor type as an output variable could also lead to the establishment of a hierarchy of the models based on the characteristics predicted, similar to what was investigated by Coble et al. [7]. Accounting for variations in the cycle history of the assemblies could include the outage length between cycles and the power level of the reactor. These changes in the cycle history result in changes in the radiation emissions, despite having the same characteristics. Including these variations in the training data set allows for investigation of how these modeling techniques can predict the desired outputs based on an increased solution space.

The use of different sets of inputs and outputs can be explored for use in characterizing and estimating fissile content in UNF. Examples include using gamma and neutron counts as inputs to directly estimate the fissile content, or using gamma and neutron counts to estimate isotopic concentrations then using those concentrations to characterize the fuel or estimate the fissile content. Each of these methods will have their own advantages and limitations, which are worth exploring to find the best method for safeguards purposes.

Finally, the application of these models to process monitoring can be explored. This encompasses comparing the measured radiation signatures at various points in a facility to expected results. Differences may indicate a diversion of material or reduced performance in the process. To assist in this extension, it may be useful to switch the inputs and the outputs of the models constructed: the inputs are the fuel characteristics, previously verified, and the outputs are the radiation signatures. The output of this model can then be compared to those measured at the facility.

Bibliography

[1] M. Stone, "Cross-Validatory Choice and Assessment of Statistical Predictions," *Journal of the Royal Statistical Society. Series B (Methodological)*, vol. 36, no. 2, pp. 111–147, 1974. Publisher: [Royal Statistical Society, Wiley]. viii, 10, 11

[2] J. Ruscio and B. Roche, "Determining the number of factors to retain in an exploratory factor analysis using comparison data of known factorial structure.," *Psychological Assessment*, vol. 24, pp. 282–292, June 2012. viii, 12, 13

[3] "Treaty on the Non-Proliferation of Nuclear Weapons (NPT) – UNODA." Library Catalog: www.un.org. 1

[4] I. A. E. A. Information Circular, "INFCIRC/153," 1972. 1, 3

[5] J. R. Phillips, "Irradiated Fuel Measurements," in *Passive Nondestructive Analysis of Nuclear Materials*, Los Alamos National Lab., NM (United States), Mar. 1991. 1, 3, 5, 6, 7, 18, 25, 68

[6] K. J. Dayman, J. B. Coble, C. R. Orton, and J. M. Schwantes, "Characterization of used nuclear fuel with multivariate analysis for process monitoring," *Nuclear Instruments and Methods in Physics Research Section A: Accelerators, Spectrometers, Detectors and Associated Equipment*, vol. 735, pp. 624 – 632, 2014. 1, 9, 14, 15, 18, 72

[7] J. Coble, C. Orton, and J. Schwantes, "Multivariate analysis of gamma spectra to characterize used nuclear fuel," *Nuclear Instruments and Methods in Physics Research Section A: Accelerators, Spectrometers, Detectors and Associated Equipment*, vol. 850, pp. 18 – 24, 2017. 1, 14, 15, 18, 52, 72, 73, 84

[8] "IAEA Safeguards Glossary," Feb. 2019. Library Catalog: www.iaea.org. 3

[9] J. R. Phillips, J. K. Halbig, D. M. Lee, S. E. Beach, T. R. Bement, E. Dermendjiev, C. R. Hatcher, K. Kaieda, and E. G. Medina, "Application of nondestructive gamma-ray and neutron techniques for the safeguarding of irradiated fuel materials," May 1980. Library Catalog: digital.library.unt.edu, Number: LA-8212. 3, 4, 5, 6, 8

[10] T. England, W. Wilson, M. Stamatelatos, L. A. S. L. T. Division, E. P. R. Institute, U. S. E. Research, and D. Administration, *Fission Product Data for Thermal Reactors: Users manual for EPRI-CINDER code and data.* Fission Product Data for Thermal Reactors, Electric Power Research Institute, 1976. 4

[11] B. T. Rearden and M. A. Jessee, "SCALE Code System," Tech. Rep. ORNL/TM–2005/39-V-6.2, Oak Ridge National Laboratory (ORNL), 2016. 4, 19

[12] D. Henzlova, H. O. Menlove, C. D. Rael, H. R. Trellue, S. J. Tobin, S.-H. Park, J.-M. Oh, S.-K. Lee, S.-K. Ahn, I.-C. Kwon, and H.-D. Kim, "Californium interrogation prompt neutron (CIPN) instrument for non-destructive assay of spent nuclear fuel—Design concept and experimental demonstration," *Nuclear Instruments and Methods in Physics Research Section A: Accelerators, Spectrometers, Detectors and Associated Equipment*, vol. 806, pp. 43–54, Jan. 2016. 4

[13] "The Agency's Safeguards System (1965)," Dec. 1965. Library Catalog: www.iaea.org. 4

[14] P. C. Durst, I. Therios, R. Bean, A. Dougan, B. Boyer, R. Wallace, M. H. Ehinger, D. N. Kovacic, and K. Tolk, "Advanced Safeguards Approaches for New Reprocessing Facilities," June 2007. Library Catalog: digital.library.unt.edu, Number:PNNL-16674. 4, 21

[15] R. E. Johns and M. Schanfein, "Chapter 7 - Nuclear Material Accounting and Control," in *Nuclear Safeguards, Security, and Nonproliferation (Second Edition)* (J. E. Doyle, ed.), pp. 157–229, Boston: Butterworth-Heinemann, Jan. 2019. 4, 5

[16] B. Bevard, J. Wagner, C. Parks, and M. Aissa, "Review of Information for Spent Nuclear Fuel Burnup Confirmation (NUREG/CR-6998)," tech. rep., U.S. NRC, Dec. 2009. 5, 6, 7, 77

[17] A. Lebrun, G. Bignan, H. Recroix, and M. Huver, "Characterization of spent fuel assemblies for storage facilities using non destructive assay," tech. rep., 1999. 6, 8

[18] C. Willman, A. Håkansson, O. Osifo, A. Bäcklin, and S. J. Svärd, "Nondestructive assay of spent nuclear fuel with gamma-ray spectroscopy," *Annals of Nuclear Energy*, vol. 33, pp. 427–438, Mar. 2006. 6, 9

[19] H. A. Smith Jr, "The measurement of uranium enrichment," in *Passive Nondestructive Analysis of Nuclear Materials*, Los Alamos National Lab., NM (United States), Mar. 1991. 7

[20] A. Favalli, D. Vo, B. Grogan, P. Jansson, H. Liljenfeldt, V. Mozin, P. Schwalbach, A. Sjöland, S. Tobin, H. Trellue, and S. Vaccaro, "Determining initial enrichment, burnup, and cooling time of pressurized-water-reactor spent fuel assemblies by analyzing passive gamma spectra measured at the clab interim-fuel storage facility in sweden," *Nuclear Inst. and Methods in Physics Research, A*, vol. 820, pp. 102–111, 2016. 8, 19

[21] J. Umali and E. Barrios, "Nonparametric Principal Components Regression," *Communications in Statistics - Simulation and Computation*, vol. 43, pp. 1797–1810, Jan 2014. Publisher: Taylor & Francis _eprint: https://doi.org/10.1080/03610918.2012.744046. 9, 30

[22] C. R. Orton, C. G. Fraga, R. N. Christensen, and J. M. Schwantes, "Proof of concept simulations of the Multi-Isotope Process monitor: An online, nondestructive, near-real-time safeguards monitor for nuclear fuel reprocessing facilities," *Nuclear Instruments and Methods in Physics Research Section A: Accelerators, Spectrometers, Detectors and Associated Equipment*, vol. 629, pp. 209–219, Feb. 2011. 9, 12, 72

[23] C. Hellesen, S. Grape, P. Jansson, S. Jacobsson Svärd, M. Åberg Lindell, and P. Andersson, "Nuclear spent fuel parameter determination using multivariate analysis of fission product gamma spectra," *Annals of Nuclear Energy*, vol. 110, pp. 886–895, Dec. 2017. 9, 14, 15, 16, 18, 29, 34, 72, 73, 77

[24] A. J. Izenman, "Reduced-rank regression for the multivariate linear model," *Journal of Multivariate Analysis*, vol. 5, pp. 248–264, June 1975. 10

[25] H. Hotelling, "Analysis of a complex of statistical variables into principal components," *Journal of Educational Psychology*, vol. 24, no. 7, pp. 498,520, 1933-10. 10, 29

[26] M. Stone and R. J. Brooks, "Continuum Regression: Cross-Validated Sequentially Constructed Prediction Embracing Ordinary Least Squares, Partial Least Squares and Principal Components Regression," *Journal of the Royal Statistical Society. Series B (Methodological)*, vol. 52, no. 2, pp. 237–269, 1990. Publisher: [Royal Statistical Society, Wiley]. 10

[27] B. Abraham and G. Merola, "Dimensionality reduction approach to multivariate prediction," *Computational Statistics & Data Analysis*, vol. 48, pp. 5–16, Jan. 2005. 10

[28] H. Akaike, *Information Theory and an Extension of the Maximum Likelihood Principle*, pp. 199–213. New York, NY: Springer New York, 1998. 11, 12

[29] R. B. Cattell, "The Scree Test For The Number Of Factors," *Multivariate Behavioral Research*, vol. 1, pp. 245–276, Apr. 1966. 12

[30] C. R. Orton, C. E. Rutherford, C. G. Fraga, and J. M. Schwantes, "The Multi-Isotope Process Monitor: Multivariate Analysis of Gamma Spectra," tech. rep., Pacific Northwest National Lab.(PNNL), Richland, WA (United States), 2011. 12, 30

[31] C. R. Orton, C. G. Fraga, R. N. Christensen, and J. M. Schwantes, "Proof of concept experiments of the multi-isotope process monitor: An online, nondestructive, near real-time monitor for spent nuclear fuel reprocessing facilities," *Nuclear Instruments and Methods in Physics Research Section A: Accelerators, Spectrometers, Detectors and Associated Equipment*, vol. 672, pp. 38–45, Apr. 2012. 13, 72

[32] W. S. Charlton, B. L. Fearey, C. W. Nakhleh, T. A. Parish, R. T. Perry, J. Poths, J. R. Quagliano, W. D. Stanbro, and W. B. Wilson, "Operator declaration verification technique for spent fuel at reprocessing facilities," *Nuclear Instruments and Methods in Physics Research Section B: Beam Interactions with Materials and Atoms*, vol. 168, pp. 98–108, May 2000. 14, 15, 16, 72, 77

[33] S. Grape, E. Branger, Z. Elter, and L. Pöder Balkeståhl, "Determination of spent nuclear fuel parameters using modelled signatures from non-destructive assay and Random Forest regression," *Nuclear Instruments and Methods in Physics Research Section A: Accelerators, Spectrometers, Detectors and Associated Equipment*, vol. 969, p. 163979, July 2020. 16, 18

[34] S. Skutnik and D. Davis, "Characterization of the non-uniqueness of used nuclear fuel burnup signatures through a mesh-adaptive direct search," *Nuclear Instruments and Methods in Physics Research Section A Accelerators Spectrometers Detectors and Associated Equipment*, vol. 817, pp. 7–18, 05 2016. 18, 22

[35] J. W. Demmel, "On condition numbers and the distance to the nearest ill-posed problem," *Numerische Mathematik*, vol. 51, pp. 251–289, May 1987. 22

[36] T. Hastie, J. Friedman, and R. Tibshirani, "Model Assessment and Selection," in *The Elements of Statistical Learning: Data Mining, Inference, and Prediction* (T. Hastie, J. Friedman, and R. Tibshirani, eds.), Springer Series in Statistics, pp. 193–224, New York, NY: Springer, 2001. 23

[37] H. H. S. Schaal and S. Vijayakumar, "Local dimensionality reduction for non-parametric regression," *Neural Process Letters*, vol. 29, pp. 109–131, 2009. https://doi.org/10.1007/s11063-009-9098-0. 24, 52, 53, 63

[38] D. Garcia-Alvarez, M. J. Fuente, and G. I. Sainz, "Fault detection and isolation in transient states using principal component analysis," *Journal of Process Control*, vol. 22, pp. 551–563, Mar. 2012. 30

[39] H. F. Kaiser, "The Application of Electronic Computers to Factor Analysis," *Educational and Psychological Measurement*, vol. 20, pp. 141–151, Apr. 1960. Publisher: SAGE Publications Inc. 39

[40] S. Wold, "Nonlinear partial least squares modelling II. Spline inner relation," *Chemometrics and Intelligent Laboratory Systems*, vol. 14, pp. 71–84, Apr. 1992. 52

[41] S. Qin and T. McAvoy, "Nonlinear pls modeling using neural networks," *Computers & Chemical Engineering*, vol. 16, no. 4, pp. 379 – 391, 1992. Neutral network applications in chemical engineering. 52, 63

[42] S. de Jong, "SIMPLS: An alternative approach to partial least squares regression," *Chemometrics and Intelligent Laboratory Systems*, vol. 18, pp. 251–263, Mar. 1993. 52, 53

[43] S. Wold, A. Ruhe, H. Wold, and I. Dunn, W. J., "The Collinearity Problem in Linear Regression. The Partial Least Squares (PLS) Approach to Generalized Inverses," *SIAM Journal on Scientific and Statistical Computing*, vol. 5, pp. 735–743, Sept. 1984. Publisher: Society for Industrial and Applied Mathematics. 53

[44] I. E. Frank and J. H. Friedman, "A Statistical View of Some Chemometrics Regression Tools," *Technometrics*, vol. 35, no. 2, pp. 109–135, 1993. Publisher: [Taylor & Francis, Ltd., American Statistical Association, American Society for Quality]. 53

[45] R. Lippmann, "An introduction to computing with neural nets," *IEEE ASSP Magazine*, vol. 4, pp. 4–22, Apr. 1987. Conference Name: IEEE ASSP Magazine. 63

Vita

Amanda Bachmann graduated from Hillsborough High School in Tampa, FL in 2015. She then moved to Knoxville, TN and earned a Bachelors of Science in Nuclear Engineering with honors from the University of Tennessee, Knoxville in May 2019. She accepted a graduate research and teaching assistant position in the Department of Nuclear Engineering at the University of Tennessee, Knoxville working with Dr. Jamie Coble. She plans to graduate with her Masters of Science in Nuclear Engineering in August 2020. After graduation she will attend the University of Illinois Urbana-Champaign to work on her PhD in Nuclear Engineering under the supervision of Dr. Kathryn Huff.